

Abstract

In this study a kinetic evaporation-condensation model was applied to assess the uncertainty in determining the volatility behaviour of organic particles from thermodenuder experiments, at conditions relevant to both ambient and laboratory measurements.

A comprehensive theoretical parametric analysis showed that re-condensation in thermodenuder experiments is highly case-dependent, being strongly determined by the combined effects of aerosol mass loading, particle size and the kinetics of condensation. Because of this dependence it is possible to find cases with either negligible or significant levels of re-condensation at high organic mass loadings, thus accounting for the diverging degrees of re-condensation reported in previous experimental and modeling studies. From this analysis it was concluded that gas denudation should generally be applied in experiments with aerosol mass loading $>30 \mu\text{g m}^{-3}$. However, thermograms may be lowered in the region below 45°C as a result of the evaporation induced by denuders for compounds with saturation concentration $C^* > 1 \mu\text{g m}^{-3}$.

A calibration curve relating C^* (saturation concentration) and T_{50} (temperature at which 50% of aerosol mass evaporates) was theoretically derived and tested to infer volatility distributions from experimental thermograms. While this approach was found to hold at equilibrium, significant underestimation of the particle volatility was found under kinetically-controlled evaporation conditions. Because thermograms obtained at ambient aerosol loading levels are most likely to show departure from equilibrium, the application of a kinetic evaporation model is more suitable for inferring volatility properties of atmospheric samples than the calibration curve approach; however, this method implies significant uncertainty, due to the sensitivity of the kinetic model to the assumption of “effective” accommodation coefficient.

Predictions of the evaporation-condensation behaviour of α -pinene SOA exhibited a large uncertainty in estimating the aerosol mass formation induced by cooling, depending on whether it was assumed that gas condensation was affected by the amorphous solid state of the particles. Evaluation of the dilution-induced evaporation of α -pinene

Uncertainties in the estimation of organic aerosols volatility

E. Fuentes and
G. McFiggans

Title Page

Abstract

Introduction

Conclusions

References

Tables

Figures

⏪

⏩

◀

▶

Back

Close

Full Screen / Esc

Printer-friendly Version

Interactive Discussion



SOA showed that the equilibrium partitioning theory underpredicts the aerosol mass concentration by a factor of between 5 and 10, with respect to kinetic calculations. Analysis in this study suggests that, the mass transfer kinetic coefficient, inclusive of diffusive kinetic limitations, is a critical unknown to both estimating the volatility properties and determining the atmospheric gas-particle partitioning of SOA.

1 Introduction

Organic aerosols comprise a significant portion of atmospheric particular matter (Hallquist et al., 2009; Jimenez et al., 2009), with a long recognised impact on both human health and global climate (Kanakidou et al., 2005; Tsigaridis and Kanakidou, 2007). They comprise primary organic aerosol (POA) emissions from sources such as fossil fuel combustion, biomass burning and diverse industrial processes, and a secondary organic aerosol (SOA) contribution formed in the atmosphere from the gas phase oxidation of volatile organic compounds (Hallquist et al., 2009). The volatility of organic aerosols largely determine the partitioning of compounds between the gas and particle phases, hence influencing the particles mass concentration, composition and size, which in turn can affect the hygroscopicity and optical properties of organic aerosols in the atmosphere (Topping et al., 2011). Accurate representation of gas-particle partitioning of semi-volatile organic compounds, and its dependence on temperature, dilution conditions and chemical transformations in the atmosphere, is required for improving prediction of the global distribution of organic aerosols.

Particle evaporation studies in dilution chambers and thermodenuder systems are increasingly being conducted to characterise the volatility distribution and evaporation behaviour of primary and secondary organic aerosols in laboratory and field measurements (Huffman et al., 2008; Saleh et al., 2008; Faulhaber et al., 2009; Grieshop et al., 2009; Cappa and Wilson, 2011). A growing number of methods are being proposed in order to infer information on the volatility and thermodynamic properties of organic aerosol compounds from the evaporation profiles derived from this type of experiments

Uncertainties in the estimation of organic aerosols volatility

E. Fuentes and
G. McFiggans

Title Page

Abstract

Introduction

Conclusions

References

Tables

Figures

⏪

⏩

◀

▶

Back

Close

Full Screen / Esc

Printer-friendly Version

Interactive Discussion



Uncertainties in the estimation of organic aerosols volatilityE. Fuentes and
G. McFiggans

Title Page

Abstract

Introduction

Conclusions

References

Tables

Figures

⏪

⏩

◀

▶

Back

Close

Full Screen / Esc

Printer-friendly Version

Interactive Discussion



(Faulhaber et al., 2009; Grieshop et al., 2009; Cappa and Wilson, 2011; Saleh et al., 2011). Some of these methods rely on the assumption that equilibrium is attained in the heating section of thermodenuder systems (Offenberg et al., 2006; Saleh et al., 2008). However, the observed dependence of thermograms on a thermodenuder's residence time indicates that equilibrium may not be attained under certain experimental conditions (An et al., 2007; Grieshop et al., 2009). Theoretical analysis of particle evaporation kinetics have shown that evaporation equilibration times in thermodenuders are highly dependent on factors such as aerosol mass loading, compound volatility and evaporation coefficient (Riipinen et al., 2010), resulting in evaporative equilibrium being attained only under laboratory conditions at organic aerosol loadings $> 200 \mu\text{g m}^{-3}$ in systems with residence time ≥ 30 s (Riipinen et al., 2010; Saleh et al., 2011). Since concentrations of organic aerosol at ambient levels are typically below $50 \mu\text{g m}^{-3}$ (Huffman et al., 2008), equilibrium is expected not to be reached in thermodenuder measurements with atmospheric samples due to the limited residence time usually applied in this systems (below 30 s). Atmospheric measurements should therefore be interpreted using a kinetic rather than an equilibrium approach, otherwise this may result in significant deviations in determining the evaporation properties of the organic aerosol (Riipinen et al., 2010; Cappa and Jimenez, 2010). The use of evaporation kinetic models imposes a strong limitation in the input requirements of the properties of constituents of the particles, since in most cases even the identity of compounds in the aerosol sample is unknown (Cappa and Jimenez, 2010). In order to avoid the limitations imposed by detailed kinetic evaporation models, Faulhaber et al. (2009) proposed a method for deriving volatility distributions from thermograms, based on an empirical relationship found between the thermodenuder temperature at which 50 % of the total mass of aerosol evaporates (T_{50}) and the organic compound vapour pressure. Because this empirical calibration curve was derived from measurements at high organic aerosol loading ($100\text{--}200 \mu\text{g m}^{-3}$) with a limited set of organic compounds, while this method seems to provide good estimations for a variety of samples, it is still uncertain that it is valid for compounds and conditions other than those used for the calibration.

Uncertainties in the estimation of organic aerosols volatilityE. Fuentes and
G. McFiggans

Title Page

Abstract

Introduction

Conclusions

References

Tables

Figures

⏪

⏩

◀

▶

Back

Close

Full Screen / Esc

Printer-friendly Version

Interactive Discussion



In addition to being used to infer volatility distribution of organic aerosols, evaporation profiles obtained from isothermal dilution and thermodenuder experiments have been recently employed to derive accommodation coefficients, by coupling measurements and kinetic modelling for compounds of known volatility (Grieshop et al., 2009; Cappa and Wilson, 2011; Saleh et al., 2011). This approach has proven useful in determining accommodation coefficients for single compounds such as dicarboxylic acids (Cappa, 2010; Saleh et al., 2011), POA mixtures such as lubricating oil (Grieshop et al., 2009; Cappa and Wilson, 2011) and amorphous solid SOA derived from α -pinene ozonolysis (Cappa and Wilson, 2011). Inconsistencies exist, however, between the evaporation coefficients estimated from isothermal dilution and thermodenuder measurements for compound mixtures like lubricating oil (Grieshop et al., 2009; Cappa and Wilson, 2011). Whether this discrepancy is a result of different volatility composition resulting from the use of different aerosol generation techniques, or to artefacts derived from the evaporation methodologies applied, is unresolved.

Re-condensation has long been considered as a potential concern for the interpretation of evaporation profiles from thermodenuder measurements, as this would lead to an underestimation of a particle's volatility (Burtscher et al., 2001; Wehner et al., 2002; Huffman et al., 2008). To minimise this effect, charcoal denuders are included in the cooling section of many standard designs, such that the semi-volatile material is removed from the gas-phase, and re-condensation is suppressed as the aerosol sample cools down (Burtscher et al., 2001; Wehner et al., 2002). Experiments by Huffman et al. (2008) have proven that sulphuric acid particles present a potential for re-condensation in thermodenuder cooling sections at aerosol loadings $\leq 50 \mu\text{g m}^{-3}$, while re-condensation for organic compounds of higher volatility than sulphuric acid, has been found to be negligible. Volatility studies on Diesel exhaust and marine aerosols with volatility tandem differential mobility analyser (VTDMA) instruments have shown insignificant re-condensation in cooling sections (Orsini et al., 1999; Sakurai et al., 2003); however, it is considered that the rate of re-condensation in these systems is lower than in thermodenuder instruments owing to the low particle

coefficients of a set of primary and secondary organic aerosol samples, with a particular emphasis on analysing the discrepancies between the evaporation rates observed in dilution and heating experiments.

2 Thermodenuder model

A diffusion-evaporation model was applied to simulate the evaporation/re-condensation of particles in a cylindrical geometry thermodenuder system. The thermodenuder configuration consists of a typical design, as illustrated in Fig. 1. The model was sequentially solved on the three sections of the thermodenuder: the heating section, where the particles are subject to evaporation; the cooling section, which is the short intermediate piece of tubing where the sample approaches ambient temperature; and the denuder section, which comprises the piece of tubing where gas-phase semi-volatile compounds are removed by a charcoal adsorber in order to avoid re-condensation. Figure 1 summarises the dimensions and residence time in each part of the design.

The thermodenuder model simulates the gain and loss of material in the condensed phase resulting from evaporation and re-condensation, respectively, the transport of the gas and the evolution of the particle diameter. The steady-state evaporation/re-condensation and diffusion of a gaseous compound through a cylindrical tube, assuming azimuthal symmetry and constant coefficient of diffusion, is defined as (Tan and Hsu, 1970):

$$v_x \frac{\partial C_i}{\partial x} + v_r \frac{\partial C_i}{\partial r} = D_i \left[\frac{1}{r} \frac{\partial}{\partial r} \left(r \frac{\partial C_i}{\partial r} \right) + \left(r \frac{\partial^2 C_i}{\partial x^2} \right) \right] + q_i \quad (1)$$

where v_x and v_r are the fluid velocity in the axial and radial directions, respectively, C_i is the gas phase mass concentration of compound i , D_i is the gas diffusion coefficient, q_i is the source/sink term for the gas phase due to particle evaporation/re-condensation,

Uncertainties in the estimation of organic aerosols volatility

E. Fuentes and
G. McFiggans

Title Page

Abstract

Introduction

Conclusions

References

Tables

Figures

⏪

⏩

◀

▶

Back

Close

Full Screen / Esc

Printer-friendly Version

Interactive Discussion



Uncertainties in the estimation of organic aerosols volatility

E. Fuentes and
G. McFiggans

Title Page

Abstract

Introduction

Conclusions

References

Tables

Figures

⏪

⏩

◀

▶

Back

Close

Full Screen / Esc

Printer-friendly Version

Interactive Discussion



and x and r are the axial and radial coordinates, respectively. Equation (1) was simplified under the assumption of negligible secondary flows and diffusion in the axial direction, such that the terms involving v_r and $\frac{\partial^2 C_i}{\partial x^2}$ are eliminated from the equation. The assumption for negligible axial diffusion is valid for Péclet number of diffusion > 100 (Turpin et al., 1993), which applies to the geometry and conditions in this study (Pe = 115). The convective term for secondary flows v_r was considered to be negligible compared to the axial velocity term in Eq. (1). This assumption will be further validated by comparing with experimental results.

The term q_i , which denotes the mass gain/loss in the gas or particle phase ($C_{p,i}$) due to evaporation or re-condensation, is defined as (Seinfeld and Pandis, 1997; Cappa, 2010):

$$q_i = v_x \frac{\partial C_i}{\partial x} = -v_x \frac{\partial C_{p,i}}{\partial x} = 2\pi N D_i d_p \Gamma (x_i C_i^* - C_i) \quad (2)$$

where N is the particle number, d_p is the particle size, Γ is the Fuchs and Sutugin (1970) correction term, defined as a function of the accommodation coefficient α , x_i is the compound mass fraction in the particle and C_i^* is the compound saturation concentration.

It should be noted that the use of an accommodation coefficient to represent all potential kinetic limitations to evaporation and condensation of organic aerosols may not be strictly physically correct as it has been largely influenced by the formulation of the evaporation model applied. As an example, the kinetics of evaporation of non-liquid particles may be expected to be greatly influenced by the diffusion coefficient through a viscous solution (e.g. Tong et al., 2011). Although such behaviour should be tested in appropriate model frameworks (Pfrang et al., 2011), kinetic limitations will be evaluated in the present work in terms of an “effective” uptake coefficient γ' , which comprises all kinetic limitations to mass transfer from the aerosol to the gas phase and vice versa. Where the kinetic limitation to evaporation and re-condensation are considered of different magnitude, the uptake coefficient is split into an evaporation coefficient (γ'_{evap})

and a re-condensation coefficient (γ'_{cond}), for the evaporation and re-condensation processes, respectively. In cases where equal evaporation and condensation coefficients are considered, the effective accommodation coefficient will be denoted as α .

The boundary conditions applied to solve Eqs. (1 and 2) in the heating and cooling sections are:

$$C_i(0, r) = C_{i0,298\text{K}(CS)} \quad (3)$$

$$\frac{\partial C_i(x, R)}{\partial x} = 0 \quad (4)$$

where R is the thermodenuder radius. The first boundary equation is a constraint for the initial concentration of the organic compounds in the gas phase. The concentration of gas at the inlet of the heating section ($C_{i0,298\text{K}}$) is defined considering that the aerosol is in equilibrium at ambient temperature, and that the distribution of the organic compounds between the gas and particle phases is defined by the adsorptive partitioning theory (Pankow, 1994). For the cooling section, the initial gas phase concentration ($C_{i0,CS}$) is given by the heating section output gas distribution. The second boundary equation is a Neumann boundary condition under the assumption of no mass losses to the walls of the system.

The boundary conditions considered to solve the diffusion-evaporation equation in the denuder section are:

$$C_i(0, r) = C_{i0,DS} \quad (5)$$

$$C_i(x, R) = 0 \quad (6)$$

The first equation defines the initial conditions for the denuder section, which are given by the output gas concentration from the cooling section, while the second equation is a Dirichlet condition defining the denuder walls as a perfect sink for the gas phase. The assumption of perfect sink implies that the gas is bound completely and irreversibly upon coming into contact with the coating material. The modeled denuder performance

Uncertainties in the estimation of organic aerosols volatility

E. Fuentes and
G. McFiggans

[Title Page](#)[Abstract](#)[Introduction](#)[Conclusions](#)[References](#)[Tables](#)[Figures](#)[⏪](#)[⏩](#)[◀](#)[▶](#)[Back](#)[Close](#)[Full Screen / Esc](#)[Printer-friendly Version](#)[Interactive Discussion](#)

therefore represents an upper limit on the efficiency of the system to remove semi-volatile gas.

The temperature distribution of the gas in the heating and cooling sections was modelled using the heat equation, under the assumptions of fully developed laminar flow and negligible secondary flows and heat transfer in the axial direction as (Campo, 2004):

$$\rho c_p v_x \frac{\partial T}{\partial x} = k \left[\frac{1}{r} \frac{\partial}{\partial r} \left(r \frac{\partial T}{\partial r} \right) \right] \quad (7)$$

The assumption of fully developed flow at the entrance of the thermodenuder was adopted, given that the entrance length for a laminar flow to become fully developed in the system under study is as short as 3 cm. The assumptions of negligible radial flow with respect to the axial velocity term and negligible heat transfer diffusion in the axial direction are validated in the next section by comparing the modelled temperature distribution with experimental temperature profiles from Huffman et al. (2008).

The heat equation in the heating and cooling sections was solved for the following boundary conditions:

$$T(0, r) = T_{0,298\text{K}(CS)} \quad (8)$$

$$T(x, R) = T_{\text{wall}} \quad (9)$$

$$\frac{\partial T}{\partial r} = 0 \quad (10)$$

where the first equation specifies ambient temperature conditions $T_{0,298\text{K}}$ for the flow at the entrance of the heating section and a cooling section initial temperature ($T_{0,CS}$) defined by the output of the heating section. The second condition specifies the wall temperature at all axial positions and the third equation states no heat losses in the system.

The velocity of the fluid was modelled as a function of the local temperature, using the definition of plug flow velocity. Because particle losses were neglected and a constant particle number profile was applied in the calculations, a plug flow velocity profile

Uncertainties in the estimation of organic aerosols volatility

E. Fuentes and
G. McFiggans

Title Page

Abstract

Introduction

Conclusions

References

Tables

Figures

⏪

⏩

◀

▶

Back

Close

Full Screen / Esc

Printer-friendly Version

Interactive Discussion



(Skeel and Berzins, 1990), and an explicit Runge-Kutta formula method, both implemented in solvers in the commercial software Matlab.

3 Fluid properties

Figure 2 illustrates the modelled axial evolution of the fluid temperature in the heating and cooling sections of a thermodenuder with dimensions and operating conditions identical to those described in Huffman et al. (2008), in comparison with experimental centerline temperature measurements provided in the cited work. The initial temperature of the fluid in the model was set equal to the fluid temperature at the inlet of the active heating zone in Huffman et al. (2008) (i.e. zone covered with heating tapes), so that the thermodenuder wall temperature could be applied as a boundary condition. The wall temperature was set to the value of maximum temperature reached by the fluid in the experimental system. As shown in Fig. 2, the modelled and experimental temperature profiles are in good agreement, thus indicating that the assumptions previously made are valid for modelling the temperature and fluid properties. Calculations at different wall temperatures indicate that, for the dimensions and operating conditions applied, the wall temperature boundary condition is reached in the centerline at ~15–20 cm from the beginning of the heating section. As an example of temperature distributions, Fig. S1 shows the temperature field in the heating section of the thermodenuder for a wall temperature of 100 °C. The temperature distribution affects both the density and, consequently, the velocity of the fluid, leading to an acceleration and deceleration of the fluid in the heating and cooling section, respectively.

4 Re-condensation: parametric analysis

A parametric sensitivity study was conducted in order to evaluate the potential of re-condensation to affect thermodenuder evaporation profiles and the subsequent

Uncertainties in the estimation of organic aerosols volatility

E. Fuentes and
G. McFiggans

Title Page

Abstract

Introduction

Conclusions

References

Tables

Figures

⏪

⏩

◀

▶

Back

Close

Full Screen / Esc

Printer-friendly Version

Interactive Discussion



Uncertainties in the estimation of organic aerosols volatility

E. Fuentes and
G. McFiggans

Title Page

Abstract

Introduction

Conclusions

References

Tables

Figures

⏪

⏩

◀

▶

Back

Close

Full Screen / Esc

Printer-friendly Version

Interactive Discussion



interpretation of thermograms. For the analysis, the influence of aerosol loading (C_{OA}), particle size (d_p), accommodation coefficient (α), volatility (C^*) and diffusion coefficient (D_i) on gas re-condensation, was evaluated by comparing thermograms obtained after the heating, cooling and denuder sections in the thermodenuder model. The output thermogram for an equivalent system without denuder section was also calculated in order to assess the level of re-condensation and the performance of the charcoal denuder. The mass fraction remaining, calculated as a function of the heater temperature, was defined as $MFR = M_f/M_0$, where M_f is the aerosol mass after the corresponding section in the thermodenuder and M_0 is the initial aerosol mass in the system (M_0 is equivalent to the mass referenced to the bypass without thermodenuder, corrected for particle losses). Because the density of the particles was assumed to be constant, the mass fraction remaining is equivalent to a volume fraction remaining. Together with the thermograms comparison, the results were also evaluated in terms of re-condensation fraction (RF) (Saleh et al., 2011), defined as the percent of evaporated gas that re-condenses onto the particles after the cooling section (C_{CS}) or the denuder section (C_{DS}) with respect to the amount of gas exiting the heating section (C_{HS}):

$$RF(\%) = \frac{C_{HS} - C_{CS(DS)}}{C_{HS}} \cdot 100 \quad (11)$$

Positive values of RF indicate that the gas evaporated in the heating section re-condenses in the cooling or denuder sections, while negative values indicate an increase in the gas concentration with respect to the amount of gas at the exit of the heating section. Negative values of the re-condensation fraction are expected if the removal of gas by denudation induces the evaporation of particles in the denuder section (Saleh et al., 2011).

For the parametric analysis, the case with $d_p = 100$ nm, $\alpha = 1$, $C^* = 0.1 \mu\text{g m}^{-3}$ and $C^* = 0.01 \mu\text{g m}^{-3}$, $C_{OA} = 400 \mu\text{g m}^{-3}$ and $D_i = 5 \times 10^{-6} \text{m}^2 \text{s}^{-1}$ was selected for the base-line conditions. The heat of vaporisation generally correlates with the saturation concentration, exhibiting an increasing value for decreasing volatility (Epstein et al., 2009).

Uncertainties in the estimation of organic aerosols volatilityE. Fuentes and
G. McFiggans

Title Page

Abstract

Introduction

Conclusions

References

Tables

Figures

⏪

⏩

◀

▶

Back

Close

Full Screen / Esc

Printer-friendly Version

Interactive Discussion



In order to apply an enthalpy of vaporisation consistent with the compound's volatility, the linear equation derived by Epstein et al. (2009) was applied. For the volatilities above indicated, this expression yields near-room temperature enthalpy values of 151 kJ mol^{-1} and 140 kJ mol^{-1} , respectively. In the model, a constant heat of vaporisation was assumed over the temperature range considered. The thermodenuder geometry applied was similar to that described in Huffman et al. (2008), with dimensions, residence times and flow as indicated in Fig. 1.

Figure 3 shows the thermograms obtained after the different thermodenuder sections for $C^* = 0.01 \mu\text{g m}^{-3}$ at diverse organic aerosol loading levels. The equilibrium evaporation thermograms have also been included for comparison. In the re-condensation process, equilibrium is achieved when the initial aerosol mass is reached, i.e. for $\text{MFR} = 1$. In agreement with results in Cappa (2010), the re-condensation fraction is highly dependent on the aerosol loading and particularly promoted at high aerosol loading levels, which are typically used in laboratory experiments (Faulhaber et al., 2009; Cappa and Wilson, 2011). The predictions indicate that an already significant re-condensation occurs in the 15 cm cooling section joining the heater and the denuder sections for organic loadings $\geq 150 \mu\text{g m}^{-3}$. In addition, the removal of gas by the denuder at high organic loadings is not sufficient to avoid further re-condensation, which in the case of $400 \mu\text{g m}^{-3}$ loading leads to the re-condensation fraction being reduced in only a $\sim 10\%$ with respect to the same length of tubing without denuder. The efficiency of the denuder to hinder re-condensation is considerably higher for lower organic loading, with reductions $\geq 45\%$ in the re-condensation fraction, with respect to the case without denuder for aerosol loadings $\leq 150 \mu\text{g m}^{-3}$. Although at $50 \mu\text{g m}^{-3}$ aerosol concentration, a less significant re-condensation occurs, removal of the denuder from the system would still lead to re-condensation fractions up to 50%, indicating the necessity of using a charcoal denuder to control re-condensation. Low re-condensation occurs without denuder at an aerosol loading of $30 \mu\text{g m}^{-3}$, (Fig. S2a) indicating that no significant modification of the thermograms is expected at atmospheric conditions below this concentration. However, because atmospheric levels can reach values up to $\sim 50 \mu\text{g m}^{-3}$

(Huffman et al., 2008), it seems beneficial to keep the denuder section as part of the system in order to minimise any artefacts induced by re-condensation.

Corresponding results for visualising the relationship between volatility and re-condensation are presented in Fig. 4. For a given MFR value, the curves for the cooling section (CS and w/o DS) indicate that the re-condensation fraction does not seem to be substantially affected by the volatility of the organic aerosol. This is a result of the lower temperatures required to achieve the same level of evaporation for high volatility compounds with respect to the low volatility cases, which leads to gradients for re-condensation of similar magnitude for compounds of different volatility. A substantial difference is, however, observed in the $C^* = 10 \mu\text{g m}^{-3}$ thermogram after the denuder section with respect to the lower volatility cases. This is a result of particle evaporation induced by gas stripping in the denuder, which is enhanced with increasing volatility and particularly affects thermograms for $C^* > 1 \mu\text{g m}^{-3}$ and temperatures below 45°C . Further analysis has shown that this effect is only important for $C^* > 1 \mu\text{g m}^{-3}$, even at low aerosol loadings (Fig. S2b). Indeed, at $50 \mu\text{g m}^{-3}$ aerosol mass, evaporation induced by denudation has been predicted to be significant for volatilities $C^* > 1 \mu\text{g m}^{-3}$ (Cappa, 2010). Because the significance of this effect is limited to a narrow range of temperatures and to high volatility compounds it is likely that the impact of denudation on thermograms is less significant for multicomponent mixtures.

As illustrated in Fig. 5, the kinetics of evaporation/re-condensation are strongly affected by the effective accommodation coefficient value. Whilst it is recognised that the accommodation coefficient should not be used to represent all possible kinetic limitations to particle equilibration, its variation can be used to investigate potential instrument responses. Results in Fig. 5 show that reductions of the accommodation coefficient by an order of magnitude leads to a $\geq 50\%$ suppression of the re-condensation fraction, with negligible re-condensation predicted for $\alpha \leq 0.01$. It is also remarkable that decreasing accommodation coefficients push the system away from attaining equilibrium and that equilibrium is not reached for $\alpha \leq 0.1$, even for the high aerosol loading used in the calculations. In the work of Saleh et al. (2011), a thermodenuder with

Uncertainties in the estimation of organic aerosols volatility

E. Fuentes and
G. McFiggans

[Title Page](#)[Abstract](#)[Introduction](#)[Conclusions](#)[References](#)[Tables](#)[Figures](#)[Back](#)[Close](#)[Full Screen / Esc](#)[Printer-friendly Version](#)[Interactive Discussion](#)

Uncertainties in the estimation of organic aerosols volatilityE. Fuentes and
G. McFiggans

Title Page

Abstract

Introduction

Conclusions

References

Tables

Figures

⏪

⏩

◀

▶

Back

Close

Full Screen / Esc

Printer-friendly Version

Interactive Discussion



on the iterative adjustment of the accommodation coefficient in order to obtain the best fit between the experimental data and the model predictions, with the best fit providing information on the degree of re-condensation. For comparison with the experimental measurements, the dimensions and operating conditions of the thermodenuder system relevant to each case were used to set the geometrical boundary conditions for the model.

Thermograms of di-carboxylic acids were modeled and compared with measurements by Faulhaber et al. (2009), as shown in Fig. 7. Diverging values of accommodation coefficient for di-carboxylic acids have been reported in the literature. Whereas a value close to unity was derived by Riipinen et al. (2006) for succinic acid, low values ~ 0.1 have been determined by Saleh et al. (2011) for adipic acid. In order to account for these diverging values, the thermograms were modeled for accommodation coefficients of 0.1 and 1. Figure 7 indicates a best agreement between succinic acid measurements and model predictions for an accommodation coefficient close to unity, while significant deviation is obtained when using an evaporation coefficient of 0.1. For this latter value, all the curves collapse on the same line due to negligible re-condensation. The model indicates that re-condensation in experiments by Faulhaber et al. (2009) was low because of the charcoal denuder hindering re-condensation, since denuder removal would have led to re-condensation fractions up to 40 %. Similar results regarding the level of re-condensation and performance of the denuder were obtained for adipic and sebacic acid thermograms in Faulhaber et al. (2009). It should be noted that although the predictions indicate a low re-condensation in these experiments because of using a charcoal denuder, high aerosol loading levels on the order of $400\text{--}650\ \mu\text{g m}^{-3}$, as those in Cappa and Wilson (2011), would have led to lower efficiency of the denuder system and to a higher re-condensation fraction.

In order to understand the discrepancy between the significant re-condensation yielded in the present study and measurements by Saleh et al. (2011) showing negligible re-condensation at high aerosol loadings, experiments conducted in the cited study to test the degree of re-condensation were reproduced with the present kinetic

optimum solution for $\alpha = 0.3$. For this accommodation coefficient, a re-condensation fraction up to $\sim 50\%$ is predicted if a denuder is not applied, indicating the need to incorporate this system in the experimental configuration.

As pointed out in previous work by Cappa and Wilson (2011), the accommodation inferred from their thermograms is in contrast to the low accommodation coefficient between 0.001–0.0001 derived from dilution experiments by Grieshop et al. (2009). Although it is likely that material released from the chamber walls can affect the kinetics of particle evaporation in chamber experiments (Matsunaga and Ziemann, 2010), it has been argued that this discrepancy may result from differences in the aerosol volatility because of using different particle generation methods (Grieshop, 2011). In order to analyse whether this is actually due to the aerosol generation technique, the evaporation model was applied to derive the accommodation coefficient from evaporation experiments conducted with a thermodenuder fed with the same lubricating oil aerosol sample used for the dilution chamber experiments in Grieshop et al. (2009) (Fig. 8b). The specifications and operation of the thermodenuder system applied were those described in An et al. (2007) and Grieshop et al. (2009), with a HS centerline residence time of 16 s for a flow of 1 lpm (32 s plug flow residence time). Note that for this thermodenuder system the denuder section was directly attached at the outlet of the heating section, thus only output thermograms for the heating section (HS) and denuder section (DS) are provided. In agreement with previous analysis on thermograms by Cappa and Wilson (2011), the model yields an accommodation coefficient value between 0.1 and 1 for the thermodenuder measurement by Grieshop et al. (2009), with an optimum fit for $\alpha = 0.3$, thus revealing the existence of a notable discrepancy in the evaporation rate of the same aerosol sample in the thermodenuder and dilution measurements by Grieshop et al. (2009). As pointed out above, the slow evaporation rate of particles in Grieshop et al. (2009) dilution chamber may be induced by the release of material from the chamber walls. Because of the potential artifact induced by the release of material from the chamber walls on particle evaporation, dilution experiments with standard Teflon walls do not seem to be an adequate methodology for conducting

Uncertainties in the estimation of organic aerosols volatility

E. Fuentes and
G. McFiggans

[Title Page](#)[Abstract](#)[Introduction](#)[Conclusions](#)[References](#)[Tables](#)[Figures](#)[Back](#)[Close](#)[Full Screen / Esc](#)[Printer-friendly Version](#)[Interactive Discussion](#)

this type of studies. For this purpose, special dilution chambers provided with activated charcoal absorber should be used (Vaden et al., 2010).

In order to analyse the evaporation/re-condensation behaviour of α -pinene SOA particles, experimental measurements by Cappa and Wilson (2011) were also simulated with the kinetic model. Assuming equal evaporation and re-condensation coefficients, a very low effective evaporation coefficient of 0.0001 is necessary to fit the model to the thermodynamic data (Cappa and Wilson, 2011). Although the slow evaporation of α -pinene SOA aerosol has been attributed to the barrier to the diffusion process due to the amorphous structure of the particles, re-condensation of gas on the particle surface may not be affected by the particle phase. In such a case, the kinetic coefficient for re-condensation could exhibit a higher value than that for the evaporation process. It should be noted that, because the kinetic limitation in reality may lie in the diffusion in the condensed phase through a viscous particle, the evaporation coefficient does not need to equal the condensation coefficient in the current model configuration. Based on this assumption, Fig. 9 illustrates the results of the model for different evaporation coefficients (γ'_{evap}) between 0.0001–1 and a re-condensation coefficient (γ'_{cond}) of unity. In agreement Cappa and Wilson (2011) in the case of equal evaporation and re-condensation coefficients, the accommodation coefficient would have a value between 0.001–0.0001 and re-condensation would be negligible. However, if the re-condensation and evaporation coefficients are allowed to be different, for a re-condensation coefficient close to unity, the evaporation coefficient would have a value close to ~ 0.01 , and a significant re-condensation could occur after the heating section. This shows that the interpretation of the behaviour of the aerosol and the estimation of the degree of re-condensation is certainly dependent on the assumption of the re-condensation process being or not affected by the amorphous solid phase of SOA and the specific values assumed for both the effective evaporation and re-condensation coefficients. It should be remarked that care must be taken not to over-interpret the roles of evaporation and re-condensation coefficients when the kinetic limitation may be mainly due to the particle phase; however, the allowable discrepancy

Uncertainties in the estimation of organic aerosols volatility

E. Fuentes and
G. McFiggans

[Title Page](#)[Abstract](#)[Introduction](#)[Conclusions](#)[References](#)[Tables](#)[Figures](#)[⏪](#)[⏩](#)[◀](#)[▶](#)[Back](#)[Close](#)[Full Screen / Esc](#)[Printer-friendly Version](#)[Interactive Discussion](#)

within experimental error of this coefficient may give an indication of the shrinkage and growth response to temperature changes of SOA particles.

Regarding the potential effect of the denuder on particle evaporation, it should be noted that the DS output thermograms do not seem to be significantly lowered in the region below $\leq 45^\circ\text{C}$ with respect to the HS output for the multicomponent aerosol compositions studied. This indicates that the re-condensation issue is still dominant for the conditions and aerosol loadings considered here. However, the induction of particle evaporation by the denuder may be more significant at atmospheric aerosol loadings, where less material is available in the gas phase. Thus, it should be taken into account that experimental thermograms may be lowered in the region below $\leq 45^\circ\text{C}$ due to the evaporation induced by the charcoal denuder.

6 The relationship between C^* and T_{50}

The empirical calibration curve derived by Faulhaber et al. (2009) has been proposed as a method to derive vapour pressure values and volatility distributions from thermograms (Cappa and Jimenez, 2010). This curve, which is based on an empirical relationship determined between the vapour pressure and the temperature at which 50 % of the aerosol mass evaporates (T_{50}), was derived from a limited set of semi-volatile organic compounds at $\sim 150 \mu\text{g m}^{-3}$ aerosol loading (Faulhaber et al., 2009). Hence, the validity of this calibration curve for compounds and conditions diverging from those used for the calibration remains to be proven. In this section, insights on the theoretical interpretation of the relationship comprising this calibration curve and on its validity for predicting the volatility of a variety of compounds are provided.

Following similar reasoning to Saleh et al. (2008), the change of particle phase mass resulting from the evaporation/condensation of a compound i by heating/cooling from an initial reference state 0 to a final state f , is considered equal to the change of gas phase mass and defined, including the kelvin effect ($K_{0(f)}$), as:

Uncertainties in the estimation of organic aerosols volatility

E. Fuentes and
G. McFiggans

Title Page

Abstract

Introduction

Conclusions

References

Tables

Figures

⏪

⏩

◀

▶

Back

Close

Full Screen / Esc

Printer-friendly Version

Interactive Discussion



$$\Delta c_{p,i} = \Delta c_{g,i} = C_{i,0}^* x_{i,0} K_0 - C_{i,f}^* x_{i,f} K_f \quad (12)$$

where $C_{i,0}^*$ and $C_{i,f}^*$ are the saturation concentration at the reference temperature (i.e. 298 K) and at the final temperature state expressed in terms of mass, respectively, and $x_{i,0}$ and $x_{i,f}$ are the mass fractions of component i in the particle phase at the reference and final states, respectively.

The Clausius-Clapeyron equation defines the vaporisation enthalpy ($H_{v,i}$) and saturation concentration relationship under the assumption of enthalpy constant over the temperature range as:

$$C_{i,f}^* = C_{i,0}^* \exp \left[\frac{-\Delta H_{v,i}}{R} \left(\frac{1}{T_0} - \frac{1}{T_f} \right) \right] \frac{T_0}{T_f} \quad (13)$$

Using the above equation, the change in particle mass can be defined from Eq. (11) as:

$$\Delta c_{p,i} = C_{i,0}^* x_{i,0} K_0 \left(\frac{x_{i,f} K_f T_0}{x_{i,0} K_0 T_f} \exp \left(-\frac{\Delta H_{v,i}}{R} \left(\frac{1}{T_f} - \frac{1}{T_0} \right) \right) - 1 \right) \quad (14)$$

By expressing the change in total particle mass in terms of C_{OA} difference, the previous equation leads to:

$$C_{OAi,0} - C_{OAi,f} = C_{i,0}^* x_{i,0} K_0 \left(\frac{x_{i,f} K_f T_0}{x_{i,0} K_0 T_f} \exp \left(-\frac{\Delta H_{v,i}}{R} \left(\frac{1}{T_f} - \frac{1}{T_0} \right) \right) - 1 \right), \quad (15)$$

which divided by $C_{OAi,0}$ yields:

Uncertainties in the estimation of organic aerosols volatility

E. Fuentes and
G. McFiggans

Title Page

Abstract

Introduction

Conclusions

References

Tables

Figures

⏪

⏩

◀

▶

Back

Close

Full Screen / Esc

Printer-friendly Version

Interactive Discussion

$$1 - \frac{C_{OAi,f}}{C_{OAi,0}} = \frac{C_{i,0}^* x_{i,0} K_0}{C_{OAi,0}} \left[\frac{x_{i,f} K_f T_0}{x_{i,0} K_0 T_f} \exp\left(-\frac{\Delta H_{v,i}}{R} \left(\frac{1}{T_f} - \frac{1}{T_0}\right)\right) - 1 \right] \quad (16)$$

Using the definition of mass fraction remaining for a component i , $MFR_i = C_{OAi,f}/C_{OAi,0}$
 Eq. (15) leads to the following expression for $C_{i,0}^*$:

$$C_{i,0}^* = \frac{1}{K_0} C_{OA,0} (1 - MFR_i) \left[\frac{x_{i,f} K_f T_0}{x_{i,0} K_0 T_f} \exp\left(-\frac{\Delta H_{v,i}}{R} \left(\frac{1}{T_f} - \frac{1}{T_0}\right)\right) - 1 \right]^{-1} \quad (17)$$

Assuming equal density of the organic compounds in the particle, the mass fraction remaining is equal to a volume fraction remaining and the kelvin term ratio can be expressed as:

$$\frac{K_f}{K_0} = \exp\left[\frac{4M_i \sigma (T_0 - T_f MFR^{1/3})}{\rho_i R T_0 T_f d \rho_0 MFR^{1/3}} \right] \quad (18)$$

with the Kelvin term K_0 in Eq. (16) defined as:

$$K_0 = \exp\left(\frac{4M_i \sigma}{RT_0 \rho d \rho_0} \right) \quad (19)$$

Using the definition of total mass fraction remaining, $MFR = C_{OA,f}/C_{OA,0}$, the mass fraction ratio can be expressed as:

$$\frac{x_{i,f}}{x_{i,0}} = \frac{MFR_i}{MFR} \quad (20)$$

Uncertainties in the estimation of organic aerosols volatility

E. Fuentes and
G. McFiggans

Title Page

Abstract

Introduction

Conclusions

References

Tables

Figures

⏪

⏩

◀

▶

Back

Close

Full Screen / Esc

Printer-friendly Version

Interactive Discussion



and Eq. (16) can be re-written as:

$$C_{i,0}^* = \frac{1}{K_0} C_{OA,0} (1 - MFR_i) \left[\frac{MFR_i K_f T_0}{MFR K_0 T_f} \exp\left(-\frac{\Delta H_{v,i}}{R} \left(\frac{1}{T_f} - \frac{1}{T_0}\right)\right) - 1 \right]^{-1} \quad (21)$$

For $MFR_i = 0.5$, $T_f = T_{50}$ and the saturation concentration C_0^* for a single component ($MFR = MFR_i$) is formulated as:

$$C_0^* = \frac{0.5}{K_0} C_{OA,0} \left[\frac{K_f T_0}{K_0 T_{50}} \exp\left(-\frac{\Delta H_{v,i}}{R} \left(\frac{1}{T_{50}} - \frac{1}{T_0}\right)\right) - 1 \right]^{-1} \quad (22)$$

In an analogous manner, the expression of C_i^* for a multicomponent mixture at $MFR_i = 0.5$ is given by:

$$C_{i,0}^* = \frac{0.5}{K_0} C_{OA,0} \left[\frac{0.5 K_f T_0}{MFR K_0 T_{50,i}} \exp\left(-\frac{\Delta H_{v,i}}{R} \left(\frac{1}{T_{50,i}} - \frac{1}{T_0}\right)\right) - 1 \right]^{-1} \quad (23)$$

Equations (22) and (23) provide expressions relating C_0^* and $1/T_{50}$, which will be compared with the empirical equation by Faulhaber et al. (2009). It should be noted that because the derived equations are based on the definition of particle mass evaporated between equilibrium states, the obtained expressions are constrained to equilibrium thermograms. The sensitivity of the equilibrium calibration curve to the aerosol properties defined within the kelvin term, was evaluated at constant aerosol loading and heat of vaporisation for dp_0 between 30–200 nm, density between 800–2000 kg m⁻³, molar mass between 100–400 g mol⁻¹ and surface tension between 0.05–0.073 mN m⁻¹. This sensitivity analysis yielded a very low influence of the above particle properties

Uncertainties in the estimation of organic aerosols volatility

E. Fuentes and
G. McFiggans

Title Page

Abstract

Introduction

Conclusions

References

Tables

Figures

⏪

⏩

◀

▶

Back

Close

Full Screen / Esc

Printer-friendly Version

Interactive Discussion

on the calibration curve, with maximum deviations of 2 °C in the estimation of T_{50} . Because of the low sensitivity of the calibration curve to the kelvin term, both K_f/K_0 and $1/K_0$ were assumed to be ~ 1 in the following calculations.

Figure 10 shows $\log(P_0)$ vs. $1/T_{50}$ values derived using the single component theoretical expression (Eq. 22), applied for the calibration compound in Faulhaber et al. (2009) (i.e. dicarboxylic acids, oleic acid and DOS aerosol). The agreement between the experimental data and theoretical results, reveals that the empirical equation derived by Faulhaber et al. (2009) is in fact the equilibrium relationship between C_0^* and $1/T_{50}$ in Eq. (22), specifically defined for the selected calibration compounds at $C_{OA,0} = 150 \mu\text{g m}^{-3}$. Indeed, when averaging the properties of enthalpy of vaporisation, molar mass and vapour pressure of the calibration compounds the equilibrium theoretical equation leads to the expression $\log(P_0) = 7376 T_{50}^{-1} - 27.73$, which is strikingly similar to the empirical expression $\log(P_0) = 8171 T_{50}^{-1} - 29.61$, derived by Faulhaber et al. (2009).

The variation of the calibration curve as a function of $C_{OA,0}$ for organic compounds of different functional groups was analysed in order to evaluate the influence of the experimental conditions on the $C_0^* - 1/T_{50}$ relationship. Figure 11 illustrates the theoretical calibration curve for aerosol loadings between 10–400 $\mu\text{g m}^{-3}$ for different organic functional groups, together with experimental data from Faulhaber et al. (2009). The thermodynamic data used as input for the analysis was obtained from diverse literature sources (Chickos and Hanshaw, 1997; Kulikov et al., 2001; Chattopadhyay and Ziemann, 2005; Donahue et al., 2011). Results in Fig. 11 show that the data for the different groups lay on the same curve, with a relatively good agreement between the empirical calibration and the theoretical curve data for $C_{OA,0}$ between 150–400 $\mu\text{g m}^{-3}$ and a more significant deviation between the empirical and theoretical curves for decreasing aerosol loading. The fact that the different type of compounds lay on the same curve at constant aerosol loading, results from the vaporisation enthalpy and C_0^* data following a relationship which is found to be equivalent to that provided by Epstein et al. (2009):

Uncertainties in the estimation of organic aerosols volatility

E. Fuentes and
G. McFiggans

[Title Page](#)[Abstract](#)[Introduction](#)[Conclusions](#)[References](#)[Tables](#)[Figures](#)[⏪](#)[⏩](#)[◀](#)[▶](#)[Back](#)[Close](#)[Full Screen / Esc](#)[Printer-friendly Version](#)[Interactive Discussion](#)

$$H_{V,i} = -11 \log(C_i^*) + 129 \quad (24)$$

Figure 11 shows that, because of the dependence of the equilibrium calibration curve on the organic aerosol loading, the aerosol volatility would be underestimated by more than one order of magnitude when applying the empirical calibration at atmospheric aerosol levels of $\sim 10 \mu\text{g m}^{-3}$, with respect to the equilibrium equation. Because of the reduced uncertainty and inclusion of all the factors affecting the C^* vs. $1/T_{50}$ relationship, the mathematical combination of the theoretical calibration curves defined in Eqs. (22) and (23) together with Eq. (24) constitute a more accurate approach for the estimation of saturation concentrations from equilibrium thermograms than the empirical expression of Faulhaber et al. (2009).

It has been shown in previous work (Riipinen et al., 2010) and in Sect. 4 of this study that equilibrium might not be attained in thermodenuders measurements at low aerosol loadings and for low effective evaporation coefficients. Hence, underestimation of particles volatility using the equilibrium calibration curve is expected at these non-equilibrium conditions. Figure 12 illustrates the deviations expected with respect to the theoretical calibration curve due to equilibrium not been attained in the thermodenuder measurements. At kinetic-controlled conditions, T_{50} would be larger than the corresponding value at equilibrium, which leads to non-equilibrium calibration curves laying on the left of the equilibrium curve, deviating from the empirical relationship according to the specific case. The deviations from the equilibrium curve due to low aerosol loading and low evaporation coefficients have been depicted in Fig. 12. Deviation of T_{50} up to 20–30 °C from the equilibrium value fortuitously places the calibration curve within the region of uncertainty of the empirical equation. Larger deviations from equilibrium situates the calibration curve at significant distance from the empirical and equilibrium curves, invalidating the general application of the empirical and theoretical curves for estimating the volatility of compounds from non-equilibrium thermograms.

Uncertainties in the estimation of organic aerosols volatility

E. Fuentes and
G. McFiggans

[Title Page](#)[Abstract](#)[Introduction](#)[Conclusions](#)[References](#)[Tables](#)[Figures](#)[⏪](#)[⏩](#)[◀](#)[▶](#)[Back](#)[Close](#)[Full Screen / Esc](#)[Printer-friendly Version](#)[Interactive Discussion](#)

The general expression in Eq. (21) can also be used to derive equilibrium thermograms, i.e. MFR as a function of the temperature, if the volatility distribution of the aerosol is known, by considering that the total mass fraction remaining can be expressed as a function of MFR_j as:

$$5 \quad MFR = \sum_{i=1}^n x_{i,0} MFR_i \quad (25)$$

where $x_{i,0}$ is the mass fraction of the compound in the particle at the reference state. According to Eq. (21) and the sensitivity analysis conducted above, equilibrium thermograms would only be determined by the volatility and vaporisation enthalpy of the individual compounds in the aerosol composition and by the specific aerosol mass loading conditions. This implies that identical thermograms should be obtained with different thermodenuders for the same aerosol sample at equal aerosol loadings, if equilibrium is attained. In contrast, dependence of thermograms on additional factors such as particle size and evaporation coefficient is expected in kinetically-controlled evaporation conditions (Faulhaber et al., 2009; Riipinen et al., 2010).

15 The equilibrium curve defined in Eq. (21) can be applied not only to interpret thermodenuder measurements but also to analyse the change in aerosol mass loading upon changes in the atmospheric temperature assuming that the aerosol reaches equilibrium. The combination of Eqs. (21), (24) and (25) constitutes a system which allows for the calculation of the variations in the aerosol mass upon changes in the temperature during convective lifting, if the composition of the aerosol at a reference temperature is known. This is in fact an alternative method to using the partitioning theory in combination with the Clausius-Clapeyron equation. This approach was used to explore the variation of the equilibrium aerosol mass with changes in the temperature and dilution ratio, in comparison with kinetically-controlled evaporation/condensation simulated with the kinetic model. Figure 13 (top) illustrates the evolution of the total mass ratio COA_f/COA_0 for lubricating oil and α -pinene SOA aerosols, taking as a reference a temperature of 25 °C and an aerosol loading of $20 \mu\text{g m}^{-3}$. For lubricating oil it was

Uncertainties in the estimation of organic aerosols volatility

E. Fuentes and
G. McFiggans

[Title Page](#)[Abstract](#)[Introduction](#)[Conclusions](#)[References](#)[Tables](#)[Figures](#)[⏪](#)[⏩](#)[◀](#)[▶](#)[Back](#)[Close](#)[Full Screen / Esc](#)[Printer-friendly Version](#)[Interactive Discussion](#)

In particular, the model points at an underestimation in the aerosol mass remaining in a factor from 5 to 10, if partitioning equilibrium theory is applied. It should be noted that the estimation of particle mass evaporated with the kinetic model is also highly sensitive to the assumption of effective evaporation coefficient, and that a better constraint of this value is required to adequately predict the changes in aerosol mass upon dilution.

7 Derivation of volatility distributions from thermodenuder measurements

Evaporation profiles from thermodenuder measurements can be applied to derive the volatility distribution using the method of Faulhaber et al. (2009). This method implies using the calibration curve between C_0^* and $1/T_{50}$, together with the thermogram measurements for the subsequent derivation of the particle fraction belonging in each C_0^* volatility bin (Faulhaber et al., 2009). In this section diverse thermograms are used to derive the volatility distributions using the equilibrium equation derived in the present study, the empirical calibration by Faulhaber et al. (2009) and the kinetic model approach applied by Cappa and Jimenez (2010). The derived distributions are compared with those obtained from using the aerosol mass fraction parameterisations determined in chamber experiments by Pathak et al. (2007) and Grieshop et al. (2009) for the aerosols on study.

7.1 Calibration curve approach: empirical and theoretical equations

The volatility distribution for lubricating oil and α -pinene SOA was derived from thermogram measurements by Grieshop et al. (2009) and Cappa and Wilson (2011) (Fig. 14), using the empirical and theoretical calibration curves according to the method described in Faulhaber et al. (2009). In addition, in order to estimate the potential deviation in the prediction due to re-condensation, thermograms after the heating section were modeled using the kinetic model and subsequently used to derive the volatility distribution.

Uncertainties in the estimation of organic aerosols volatility

E. Fuentes and
G. McFiggans

Title Page

Abstract

Introduction

Conclusions

References

Tables

Figures

⏪

⏩

◀

▶

Back

Close

Full Screen / Esc

Printer-friendly Version

Interactive Discussion



volatility distribution.

For the α -pinene SOA volatility study, the cases of 1) equal evaporation and re-condensation kinetic coefficients with a mean value of 0.00055, and 2) independent coefficients for evaporation and re-condensation, with $\gamma'_{\text{evap}} = 0.0055$ and $\gamma'_{\text{cond}} = 1$ were considered. As explained in Sect. 5.2, the second case represents the evaporation of a glass-like SOA, whose re-condensation process is not limited by the particle phase and presents a re-condensation coefficient close to unity. For the first case (Fig. 15a), the thermogram is very far from equilibrium (Fig. 9), because of the low accommodation coefficient, which leads to substantial underestimation of the volatility when using both the theoretical and empirical calibration curves. In this case, the prediction using both calibration equations is similar, due the curves becoming closer at high aerosol loadings, as previously shown. For unequal evaporation and re-condensation kinetic coefficients (Fig. 15b), the distribution obtained for the case without re-condensation indicates that the prediction using the calibration curves deviates substantially from the literature distribution due to the fact that equilibrium is not reached and also because the thermogram is strongly affected by re-condensation (Fig. 9). The analysis presented here indicates that the interpretation of thermograms and prediction of volatility distributions from thermodenuder measurements is strongly affected by the assumption of equilibrium and the degree of disequilibrium resulting from kinetic limitation.

7.2 Kinetic model approach

The kinetic evaporation/re-condensation model was also applied to derive the aerosol volatility distribution from thermograms, following the approach of Cappa and Jimenez (2010). This method consists of the iterative estimation of the volatility basis set distributions by bringing into agreement the modeled and experimental thermograms, under the assumption that the total organic mass in each of the volatility bin scales with C_0 following an exponential law relationship (Cappa and Jimenez, 2010). Because this method requires specifying the accommodation coefficient, the volatility distributions inferred here were compared for a set of accommodation coefficient values, assuming

Uncertainties in the estimation of organic aerosols volatility

E. Fuentes and
G. McFiggans

Title Page

Abstract

Introduction

Conclusions

References

Tables

Figures

◀

▶

◀

▶

Back

Close

Full Screen / Esc

Printer-friendly Version

Interactive Discussion



Uncertainties in the estimation of organic aerosols volatilityE. Fuentes and
G. McFiggans

Title Page

Abstract

Introduction

Conclusions

References

Tables

Figures

⏪

⏩

◀

▶

Back

Close

Full Screen / Esc

Printer-friendly Version

Interactive Discussion



equal kinetic coefficients for evaporation and re-condensation. Figure 16 shows the volatility distributions derived from the α -pinene SOA aerosol thermogram by applying the kinetic model (results of the fitting between model and measurements are presented in Fig. S6). The thermodenuder measurements for α -pinene SOA could not be adequately fitted with the model for accommodation coefficients above 0.01, thus constraining these parameters to values ≤ 0.01 . The volatility distributions obtained with this method are highly sensitive to the assumption of kinetic coefficient. In this particular case, an overestimation and underestimation of the volatility is obtained for accommodation coefficients values of 0.0001 and 0.01, respectively, while a reasonable agreement between the literature and estimated volatility distributions is obtained for an evaporation coefficient of 0.001.

Volatility distributions for different groups of atmospheric organic aerosols, using a kinetic model, have been provided as an estimation for $\alpha = 1$ (Cappa and Jimenez, 2010). It should be taken into account that it is unknown whether the different organic groups comprising atmospheric aerosols would present different effective kinetic coefficients. This implies a large uncertainty in interpreting the volatility distribution of organic aerosols and brings into question the volatility grading scale established for different organic compound groups by Cappa and Jimenez (2010). The fact that atmospheric measurements with thermodenuders will most likely not be at equilibrium poses a strong difficulty to accurately derive the volatility properties of aerosols from these type of measurements, as long as deviations from equilibrium are not more accurately constrained. Indeed, current uncertainty in determining volatility distributions for atmospheric samples will affect estimations of organic particle partitioning in atmospheric models, as well as the analysis of the role of co-condensation on organic aerosol droplet activation (Topping and McFiggans, 2011).

8 Summary and conclusions

In the present study a kinetic evaporation-condensation model was applied to analyse the uncertainty in estimating and interpreting the evaporation behaviour and volatility of aerosols from thermodenuder experiments.

Re-condensation was evaluated as a source of uncertainty for determining aerosol volatility distributions from thermodenuder measurements, because of its potential to affect thermograms. A parametric analysis showed that the re-condensation yield is highly determined by the combined effects of aerosol loading, particle size and accommodation coefficients. This dependence results in either important or negligible re-condensation at higher aerosol mass loadings, depending on the thermodenuder configuration and the properties of the aerosol sample. These findings reconcile previous works reporting diverging degrees of re-condensation and suggest that denuder sections should be kept in thermodenuder systems for aerosol loadings $>30 \mu\text{g m}^{-3}$, as a prevention for those conditions in which re-condensation may be significant. Analysis of the effect of denuders on particle evaporation indicated that experimental thermograms may be lowered in the region below 45°C as a result of evaporation induced by the charcoal denuder at atmospheric aerosol levels.

Estimation of effective accommodation coefficient values from experimental evaporation measurements with lubricating oil aerosol revealed the existence of artefacts in the evaporation occurring in standard chamber dilution experiments, which is manifested as a notable deceleration of the particle evaporation rate, presumably resulting from the release of material from the chamber walls. From this analysis it is concluded that dilution experiments with standard Teflon walls do not seem to be an adequate methodology for conducting this type of studies.

Theoretical derivation of the empirical calibration curve between the saturation concentration C^* and temperature at which 50% of the particle mass evaporates (T_{50}) (Faulhaber et al., 2009), revealed that this relationship is based on the change in particle mass between equilibrium temperature states, expressed explicitly as a function of C^* through the Clausius-Clapeyron equation. Calibration curve equations for a single

Uncertainties in the estimation of organic aerosols volatility

E. Fuentes and
G. McFiggans

Title Page

Abstract

Introduction

Conclusions

References

Tables

Figures

⏪

⏩

◀

▶

Back

Close

Full Screen / Esc

Printer-friendly Version

Interactive Discussion



component and multicomponent mixtures were theoretically derived and applied to estimate volatility distributions from equilibrium thermograms. Significant underestimation of the particle volatility resulted, however, when using the equilibrium calibration curve at kinetically-controlled evaporation conditions. Because thermograms obtained at ambient aerosol loading levels would likely deviate from equilibrium, a kinetic approach constitutes a more adequate method to correctly interpret the particle evaporation behaviour of atmospheric samples. However, the application of the kinetic model approach to derive volatility distributions confers significant uncertainty, owing to sensitivity of the method to the assumption of evaporation coefficient.

Analysis in this study points at the effective accommodation coefficient as a critical unknown to both determining the volatility properties of atmospheric samples and determining the atmospheric dynamics of SOA. Simulation of the evaporation-condensation behaviour of glassy α -pinene SOA, pointed at a large uncertainty in estimating the aerosol mass formation induced by cooling, depending on whether or not it is assumed that gas condensation is affected by the amorphous solid state of the particles. Analysis of dilution-induced evaporation of α -pinene SOA indicated an underprediction of the aerosol mass in a factor from 5 to 10, when using equilibrium partitioning theory with respect to the kinetic calculations for an effective evaporation coefficient between 0.01–0.0001. Predictions with the kinetic model were found to be highly sensitive to the assumption of effective evaporation coefficient. Better constraints on this parameter are therefore required to model the particle mass variation upon atmospheric dilution and cooling for glass-like SOA. Current modules to predict SOA formation in the atmosphere are based on empirically-derived mass fraction parameterisations (e.g. Strader et al., 1999) and do not account for kinetic limitations to evaporation/condensation of amorphous SOA. This study demonstrates that it is necessary to use kinetic approaches (including estimations of accommodation coefficients), alongside volatility information, to implement reasonable gas-aerosol partitioning modules in transport models that include glass-like SOA.

Uncertainties in the estimation of organic aerosols volatility

E. Fuentes and
G. McFiggans

[Title Page](#)[Abstract](#)[Introduction](#)[Conclusions](#)[References](#)[Tables](#)[Figures](#)[Back](#)[Close](#)[Full Screen / Esc](#)[Printer-friendly Version](#)[Interactive Discussion](#)

Supplementary material related to this article is available online at:
[http://www.atmos-meas-tech-discuss.net/4/6723/2011/
amtd-4-6723-2011-supplement.pdf](http://www.atmos-meas-tech-discuss.net/4/6723/2011/amtd-4-6723-2011-supplement.pdf).

Acknowledgements. This work was supported by the UK Natural Environment Research Council (grant number NE/H002561/1).

References

- An, W. J., Pathak, R. K., Lee, B. H., and Pandis, S. N.: Aerosol volatility measurement using an improved thermodenuder: application to secondary organic aerosol, *J. Aerosol Sci.*, **38**, 305–314, 2007. 6726, 6741, 6769
- Burtscher, H., Baltensperger, U., Bukowiecki, N., Cohn, P., Hüglin, C., Mohr, M., Matter, U., Nyeki, S., Schmatloch, V., Streit, N., and Weingartner, E.: Separation of volatile and non-volatile aerosol fractions by thermodesorption: instrumental development and applications, *J. Aerosol Sci.*, **32**, 427–442, 2001. 6727
- Campo, A.: On the asymptotic solution of the Graetz-Nusselt problem for short $x \rightarrow 0$ and Large $x \rightarrow \infty$ with partial usage of finite differences, *Numer. Meth. Part. D. E.*, **20**, 6, 820–830, 2004. 6732
- Cappa, C. D.: A model of aerosol evaporation kinetics in a thermodenuder, *Atmos. Meas. Tech.*, **3**, 579–592, doi:10.5194/amt-3-579-2010, 2010. 6727, 6728, 6730, 6736, 6737
- Cappa, C. D. and Jimenez, J. L.: Quantitative estimates of the volatility of ambient organic aerosol, *Atmos. Chem. Phys.*, **10**, 5409–5424, doi:10.5194/acp-10-5409-2010, 2010. 6726, 6743, 6751, 6753, 6754
- 6725, 6726, 6727, 6728, 6736, 6738, 6739, 6740, 6741, 6742, 6750, 6751, 6769, 6770
- Cappa, C. D. and Wilson, K. R.: Evolution of organic aerosol mass spectra upon heating: implications for OA phase and partitioning behavior, *Atmos. Chem. Phys.*, **11**, 1895–1911, doi:10.5194/acp-11-1895-2011, 2011.
- Chattopadhyay, S. and Ziemann, P. J.: Vapor pressures of substituted and unsubstituted monocarboxylic and dicarboxylic acids measured using an improved thermal desorption particle 25 beam mass spectrometry method, *Aerosol Sci. Tech.*, **39**, 1085–1100, 2005. 6747

Uncertainties in the estimation of organic aerosols volatility

E. Fuentes and
G. McFiggans

Title Page

Abstract

Introduction

Conclusions

References

Tables

Figures

⏪

⏩

◀

▶

Back

Close

Full Screen / Esc

Printer-friendly Version

Interactive Discussion



Uncertainties in the estimation of organic aerosols volatilityE. Fuentes and
G. McFiggans

Title Page

Abstract

Introduction

Conclusions

References

Tables

Figures

◀

▶

◀

▶

Back

Close

Full Screen / Esc

Printer-friendly Version

Interactive Discussion



- Pathak, R. K., Presto, A. A., Lane, T. E., Stanier, C. O., Donahue, N. M., and Pandis, S. N.: Ozonolysis of α -pinene: parameterization of secondary organic aerosol mass fraction, *Atmos. Chem. Phys.*, 7, 3811–3821, doi:10.5194/acp-7-3811-2007, 2007. 6740, 6751, 6776, 6777
- 5 Pfrang, C., Shiraiwa, M., and Pöschl, U.: Chemical ageing and transformation of diffusivity in semi-solid multi-component organic aerosol particles, *Atmos. Chem. Phys.*, 11, 7343–7354, doi:10.5194/acp-11-7343-2011, 2011. 6730
- Riipinen, I., Svenningsson, B., Bilde, M., Gaman, A., Lehtinen, K. E. J., and Kulmala, M.: A method for determining thermophysical properties of organic material in aqueous solu-
- 10 tions: succinic acid, *Atmos. Res.*, 82, 579–590, 2006. 6739
- Riipinen, I., Pierce, J. R., Donahue, N. M., and Pandis, S. N.: Equilibration time scales of organic aerosol inside thermodenuders: evaporation kinetics versus thermodynamics, *Atmos. Environ.*, 44, 597–607, 2010. 6726, 6748, 6749, 6766
- Sakurai, H., Park, K., McMurry, P., Zarling, D., Kittelson, D., and Ziemann, P.: Size-dependent
- 15 mixing characteristics of volatile and nonvolatile components in diesel exhaust aerosols, *Environ. Sci. Technol.*, 37, 5487–5495, 2003. 6727
- Saleh, R., Walker, J., and Khlystov, A.: Determination of saturation pressure and enthalpy of vaporisation of semi-volatile aerosols: the integrated volume method, *J. Aerosol Sci.*, 39, 876–887, 2008. 6725, 6726, 6743
- 20 Saleh, R., Shihadeh, A., and Khlystov, A.: On transport phenomena and equilibration time scales in thermodenuders, *Atmos. Meas. Tech.*, 4, 571–581, doi:10.5194/amt-4-571-2011, 2011. 6726, 6727, 6728, 6735, 6737, 6739, 6740
- Shimada, M., Seto, T., and Okuyama, K.: Thermophoretic and evaporational losses of ultrafine particles in heated flow, *AIChE J.*, 39, 1859–1869, 1993. 6733
- 25 Seinfeld, J. H. and Pandis, S. N.: *Atmospheric Chemistry and Physics: From Air Pollution to Climate Change*, Wiley-Interscience, ISBN 0471178160, New York, USA, 1997. 6730
- Skeel, R. D. and Berzins, M.: A method for the spatial discretization of parabolic equations in one space variable, *SIAM J. Sci. Stat. Comp.*, 11, 1–32, 1990. 6734
- Strader, R., Lurmann, F., and Pandis, S. N.: Evaluation of secondary organic aerosol formation
- 30 in winter, *Atmos. Environ.*, 33, 4849–4863, 1999. 6756
- Tan, C. W. and Hsu, C.-J.: Mass transfer of decaying products with axial diffusion in cylindrical tubes, *Int. J. Heat Mass Tran.*, 13, 1887–1905, 1970. 6729

Uncertainties in the estimation of organic aerosols volatilityE. Fuentes and
G. McFiggans

Title Page

Abstract

Introduction

Conclusions

References

Tables

Figures

◀

▶

◀

▶

Back

Close

Full Screen / Esc

Printer-friendly Version

Interactive Discussion

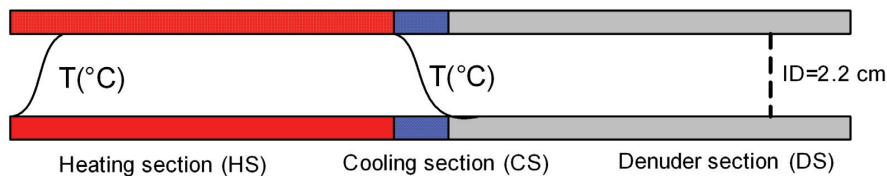


- Tong, H.-J., Reid, J. P., Bones, D. L., Luo, B. P., and Krieger, U. K.: Measurements of the timescales for the mass transfer of water in glassy aerosol at low relative humidity and ambient temperature, *Atmos. Chem. Phys.*, 11, 4739–4754, doi:10.5194/acp-11-4739-2011, 2011. 6730
- 5 Topping, D. and McFiggans, G.: Tight coupling of particle size and composition in atmospheric cloud droplet activation, *Atmos. Chem. Phys. Discuss.*, 11, 25155–25171, doi:10.5194/acpd-11-25155-2011, 2011. 6754
- Topping, D. O., Barley, M. H., and McFiggans, G.: The sensitivity of Secondary Organic Aerosol component partitioning to the predictions of component properties – Part 2: Determination of particle hygroscopicity and its dependence on “apparent” volatility, *Atmos. Chem. Phys.*, 10 11, 7767–7779, doi:10.5194/acp-11-7767-2011, 2011. 6725
- Tsigaridis, K. and Kanakidou, M.: Secondary organic aerosol importance in the future atmosphere, *Atmos. Environ.*, 41, 4682–4692, 2007. 6725
- 15 Turpin, B. J., Liu, S. P., Podolske, K. S., Gomes, M. S. P., Eisenreich, S. J., and McMurry, P. H.: Design and evaluation of a novel diffusion separator for measuring gas/particle distributions of semivolatile organic compounds, *Environ. Sci. Technol.*, 27, 2441–2449, 1993. 6730
- Vaden, T. D., Song, C., Zaveri, R. A., Imre, D., and Zelenyuk, A.: Morphology of mixed primary and secondary organic particles and the adsorption of spectator organic gases during aerosol formation, *P. Natl. Acad. Sci. USA*, 107, 6658–6663, 2010. 6742
- 20 Wehner, B., Philippin, S., and Wiedensohler, A.: Design and calibration of a thermodenuder with an improved heating unit to measure the size-dependent volatile fraction of aerosol particles, *J. Aerosol Sci.*, 33, 1087–1093, 2002. 6727

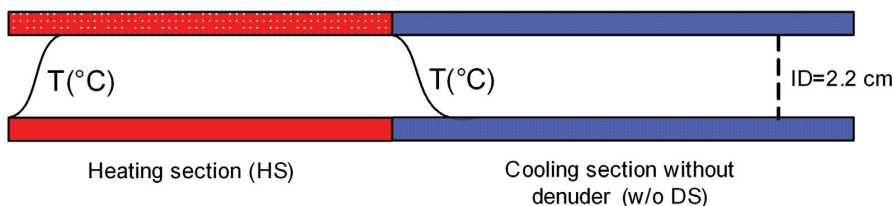
Uncertainties in the estimation of organic aerosols volatility

E. Fuentes and
G. McFiggans

Thermodenuder model : standard configuration



Thermodenuder model : denuder bypass configuration



HS	50 cm (19 s Plug flow RT, 25°C)
CS	15 cm (5.7 s Plug flow RT, 25°C)
DS	50 cm (19 s Plug flow RT, 25°C)
w/o DS	65 cm (24.7 s Plug flow RT, 25°C)

Fig. 1. Schematic of the thermodenuder design used for the calculations. The configuration with denuder bypass was also calculated to explore the potential for re-condensation and the efficiency of the charcoal denuder. Air flow = 0.6 lpm, RT = residence time.

[Title Page](#)
[Abstract](#)
[Introduction](#)
[Conclusions](#)
[References](#)
[Tables](#)
[Figures](#)
[⏪](#)
[⏩](#)
[◀](#)
[▶](#)
[Back](#)
[Close](#)
[Full Screen / Esc](#)
[Printer-friendly Version](#)
[Interactive Discussion](#)

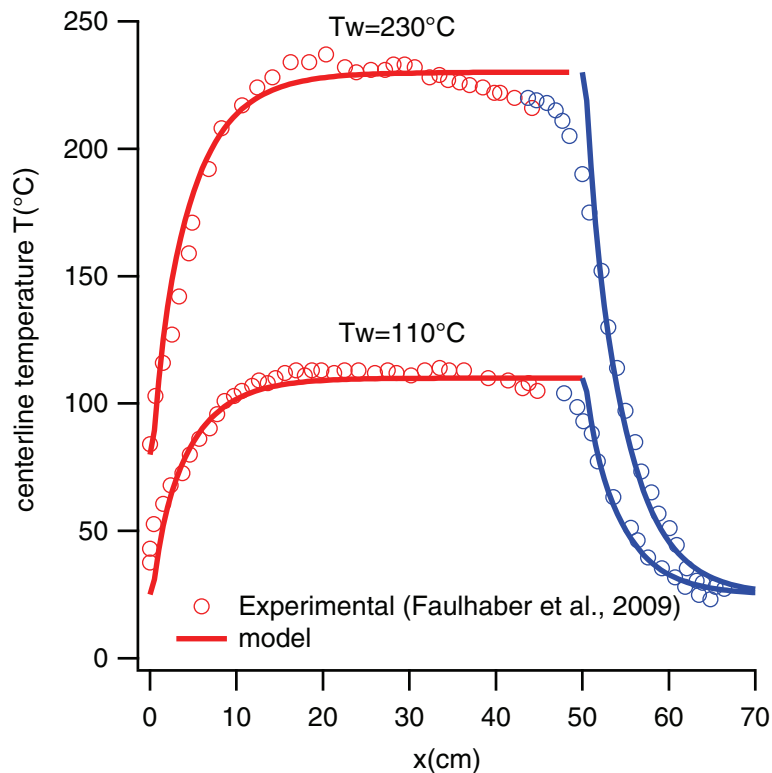


Fig. 2. Modelled and experimental centerline temperature in the heating and cooling sections of Faulhaber et al. (2009) thermodenuder. Note that the initial fluid temperature in this calculation is the centerline temperature at the inlet of the active heating zone (i.e. tube covered with heating tapes) (Faulhaber et al., 2009).

Uncertainties in the estimation of organic aerosols volatility

E. Fuentes and G. McFiggans

Title Page

Abstract Introduction

Conclusions References

Tables Figures

⏪ ⏩

◀ ▶

Back Close

Full Screen / Esc

Printer-friendly Version

Interactive Discussion



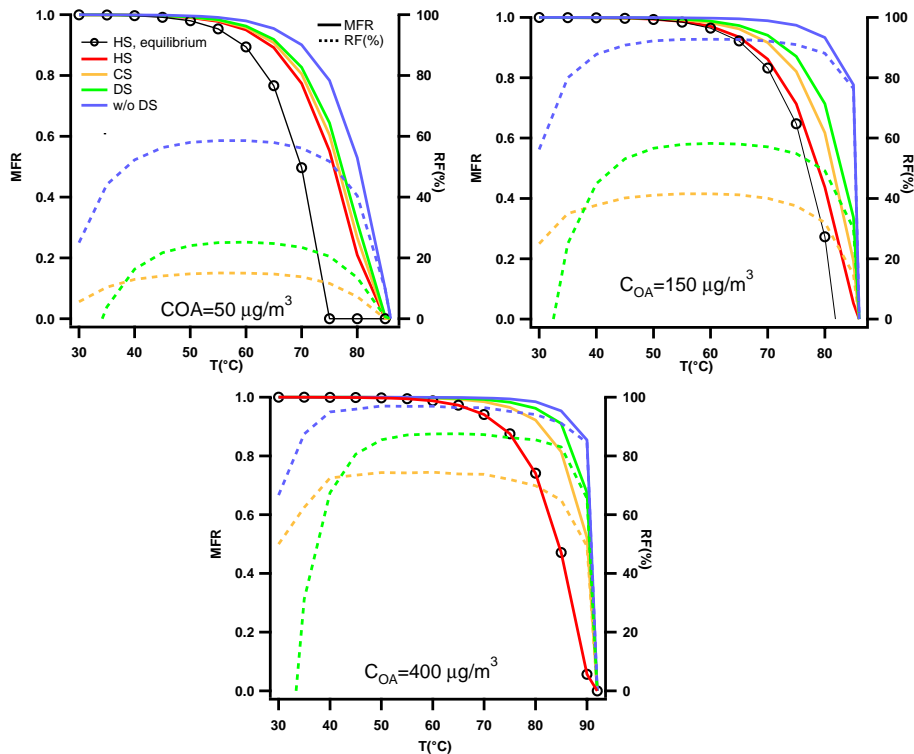


Fig. 3. Output thermograms and recondensation fraction for the heating section (HS), cooling section (CS), denuder section (DS) and equivalent configuration without denuder section (w/o DS) for different aerosol mass loadings. The re-condensation fraction (RF) indicates the percentage of gas phase mass that re-condenses with respect to the gas concentration at the exit of the heating section. The results show that the efficiency of the denuder to hinder recondensation decreases with increasing aerosol mass loading. Thermograms after the heating section approach equilibrium for high aerosol loadings. Baseline case: $C^* = 0.01 \mu\text{g m}^{-3}$, $d_p = 100 \text{ nm}$, $D_i = 5 \times 10^{-6} \text{ cm}^2 \text{ s}^{-1}$ and $\alpha = 1$.

Uncertainties in the estimation of organic aerosols volatility

E. Fuentes and G. McFiggans

Title Page

Abstract Introduction

Conclusions References

Tables Figures

⏪ ⏩

⏴ ⏵

Back Close

Full Screen / Esc

Printer-friendly Version

Interactive Discussion



Uncertainties in the estimation of organic aerosols volatility

E. Fuentes and
G. McFiggans

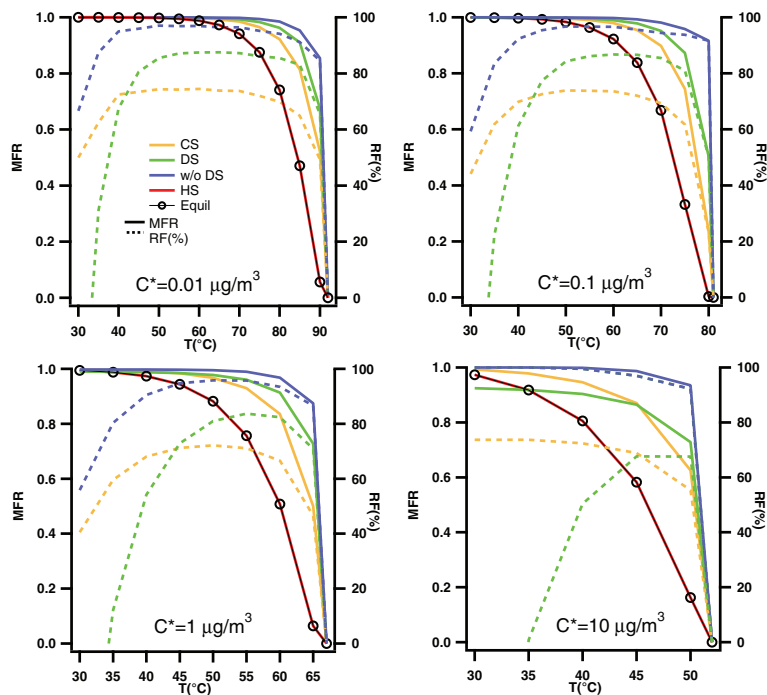


Fig. 4. Output thermograms and recondensation fraction for the heating section (HS), cooling section (CS), denuder section (DS) and equivalent configuration without denuder section (w/o DS) at different volatilities. Similar magnitude in the re-condensation fraction between the different volatility cases is obtained at equal MFR, due to the increase in volatility being counteracted by the low equilibrium saturation concentrations at low temperatures. The charcoal denuder is predicted to substantially influence thermograms only for $C^* > 1 \mu\text{g m}^{-3}$ and temperatures below 45°C , by inducing particle evaporation. Baseline case: $C_{\text{OA}} = 400 \mu\text{g m}^{-3}$, $d_p = 100 \text{ nm}$, $D_i = 5 \times 10^{-6} \text{ cm}^2 \text{ s}^{-1}$ and $\alpha = 1$.

[Title Page](#)
[Abstract](#)
[Introduction](#)
[Conclusions](#)
[References](#)
[Tables](#)
[Figures](#)
[◀](#)
[▶](#)
[◀](#)
[▶](#)
[Back](#)
[Close](#)
[Full Screen / Esc](#)
[Printer-friendly Version](#)
[Interactive Discussion](#)

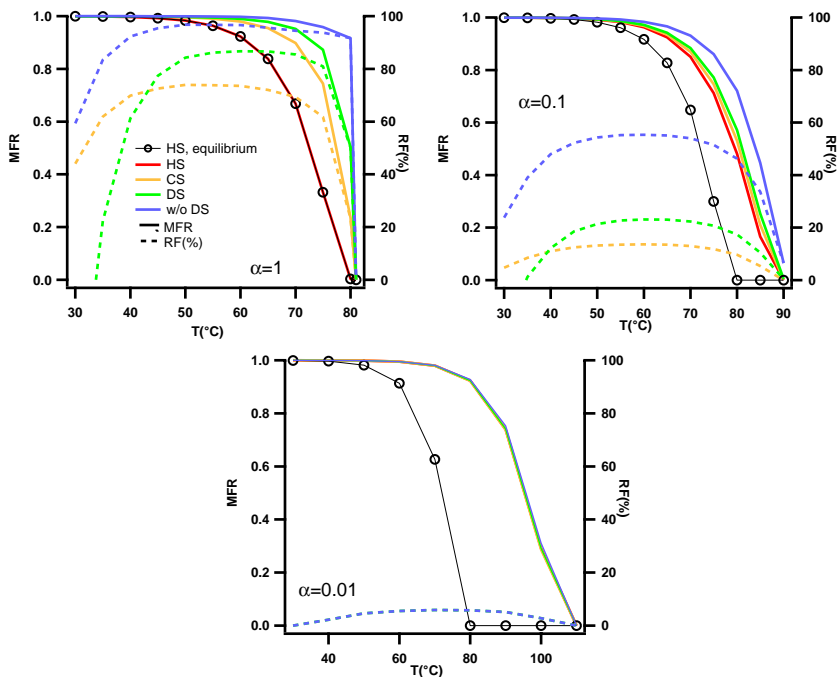


Fig. 5. Output thermograms and recondensation fraction for the heating section (HS), cooling section (CS), denuder section (DS) and equivalent configuration without denuder section (w/o DS) at different accommodation coefficients. The results indicate a strong dependence of the re-condensation rate on the accommodation coefficient, leading to a strong re-condensation for $\alpha = 1$ and negligible change in the thermograms for $\alpha \leq 0.01$. Consistent with Riipinen et al. (2010), low accommodation coefficients lead to substantial deviations from equilibrium in the evaporation process. Results shown here indicate that for accommodations coefficients $\alpha \leq 0.1$, equilibrium will not be attained in thermodenuder systems with room temperature plug flow residence time of ~ 16 s even at high aerosol mass loadings. Baseline case: $C_{OA} = 400 \mu\text{g m}^{-3}$, $C^* = 0.1 \mu\text{g m}^{-3}$, $d_p = 100 \text{ nm}$ and $D_i = 5 \times 10^{-6} \text{ cm}^2 \text{ s}^{-1}$.

Uncertainties in the estimation of organic aerosols volatility

E. Fuentes and
G. McFiggans

Title Page

Abstract

Introduction

Conclusions

References

Tables

Figures

◀

▶

◀

▶

Back

Close

Full Screen / Esc

Printer-friendly Version

Interactive Discussion

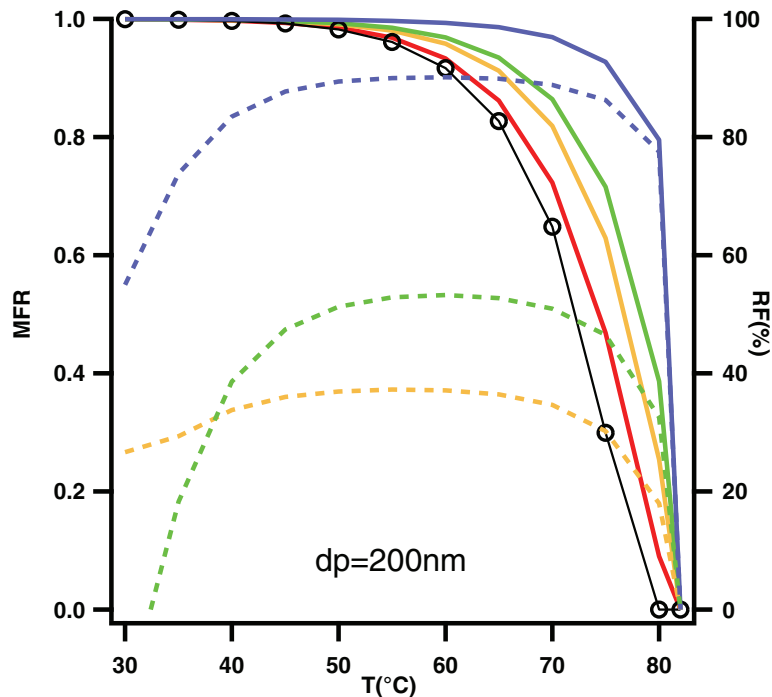


Fig. 6. Output thermograms and recondensation fraction for the heating section (HS), cooling section (CS), denuder section (DS) and equivalent configuration without denuder section (w/o DS), in a system with 200 nm aerosol particle size at $400 \mu\text{g m}^{-3}$ aerosol loading. Comparison of this plot with Fig. 5 at $\alpha = 1$ ($d_p = 100 \text{ nm}$) indicates a deceleration in the re-condensation process for increasing particle size, at constant aerosol loading. This is a result of a reduction in the particle number available, which leads to slower evaporation and re-condensation rates. Baseline case: $C^* = 0.1 \mu\text{g m}^{-3}$, $\alpha = 1$ and $D_i = 5 \times 10^{-6} \text{ cm}^2 \text{ s}^{-1}$.

Uncertainties in the estimation of organic aerosols volatility

E. Fuentes and G. McFiggans

Title Page

Abstract

Introduction

Conclusions

References

Tables

Figures

⏪

⏩

◀

▶

Back

Close

Full Screen / Esc

Printer-friendly Version

Interactive Discussion



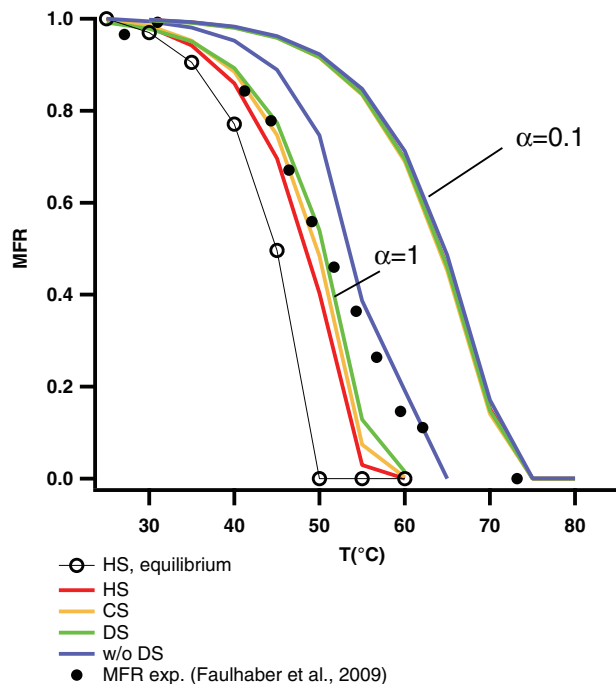


Fig. 7. Output thermograms and recondensation fraction for the heating section (HS), cooling section (CS), denuder section (DS) and equivalent configuration without denuder section (w/o DS), in a system with 200 nm butanedioic particles at $150 \mu\text{g m}^{-3}$ aerosol loading, in comparison with experiments by Faulhaber et al. (2009). The results show a best fit between observations and model for an accommodation coefficient close to unity. For this case, the inclusion of a denuder section (DS) efficiently reduces the re-condensation fraction in 40% with respect to the same length of tubing without charcoal denuder (w/o DS).

Uncertainties in the estimation of organic aerosols volatility

E. Fuentes and G. McFiggans

Title Page

Abstract Introduction

Conclusions References

Tables Figures

⏪ ⏩

⏴ ⏵

Back Close

Full Screen / Esc

Printer-friendly Version

Interactive Discussion



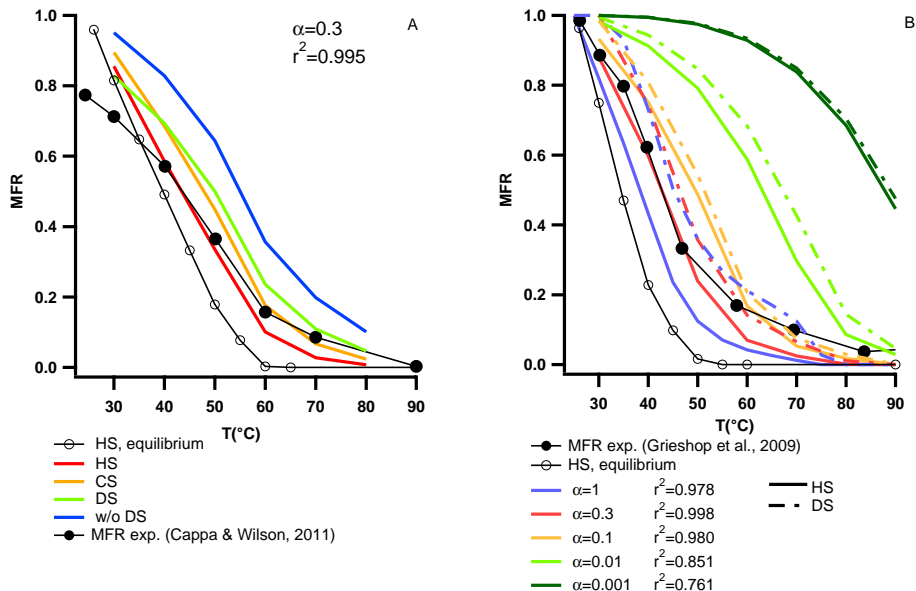


Fig. 8. (A) Output thermograms for the heating section (HS), cooling section (CS) and denuder section (DS) in a system with 240 nm lubricating oil particles at $650 \mu\text{g m}^{-3}$ aerosol loading, in comparison with experiments by Cappa and Wilson (2011). The thermodenuder system was configured as described in Cappa and Wilson (2011). **(B)** Thermograms reproducing experiments by Grieshop et al. (2009) with 175 nm lubricating oil particles at $70 \mu\text{g m}^{-3}$ aerosol loading, in comparison with experimental results. Note that for this system the denuder section was directly attached at the outlet of the heating section and only output thermograms for the heating section (HS) and denuder section (DS) are provided. The specifications and operation of the thermodenuder system were as described in An et al. (2007) and Grieshop et al. (2009). In both type of experiments **(A and B)** the results show a best fit between observations and model for an accommodation coefficient between 0.1–1, with an optimum for $\alpha = 0.3$.

Uncertainties in the estimation of organic aerosols volatility

E. Fuentes and G. McFiggans

Title Page

Abstract Introduction

Conclusions References

Tables Figures

◀ ▶

◀ ▶

Back Close

Full Screen / Esc

Printer-friendly Version

Interactive Discussion



Uncertainties in the estimation of organic aerosols volatility

E. Fuentes and
G. McFiggans

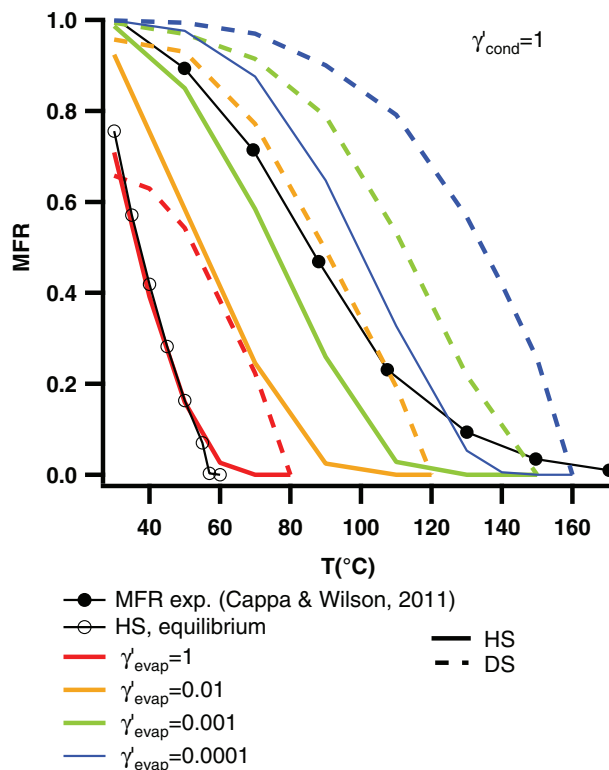


Fig. 9. Output thermograms for heating section (HS) and denuder section (DS) in a system with 92 nm α -pinene SOA particles at $500 \mu\text{g m}^{-3}$ aerosol loading, in comparison with experiments by Cappa and Wilson (2011). The calculations were conducted for different evaporation coefficients (γ'_{evap}) and a re-condensation coefficient (γ'_{cond}) close to unity, under the assumption that the particle phase does not affect the re-condensation process. The results show a best fit between observations and model for an evaporation coefficient between 0.01–0.001, with an optimum for $\alpha = 0.01$.

[Title Page](#)
[Abstract](#)
[Introduction](#)
[Conclusions](#)
[References](#)
[Tables](#)
[Figures](#)
[◀](#)
[▶](#)
[◀](#)
[▶](#)
[Back](#)
[Close](#)
[Full Screen / Esc](#)
[Printer-friendly Version](#)
[Interactive Discussion](#)

Uncertainties in the estimation of organic aerosols volatility

E. Fuentes and
G. McFiggans

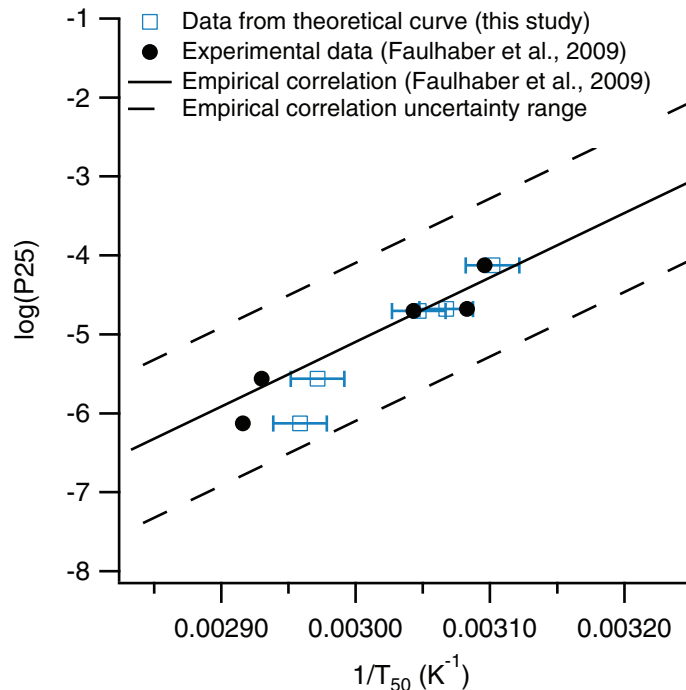


Fig. 10. Relationship between $\log P_{25}$ and $1/T_{50}$ derived with Eq. (22) for the organic compounds used in the calibration by Faulhaber et al. (2009), in comparison with experimental data. The error bars in the theoretical calculation denotes the uncertainty in the aerosol loading ($100\text{--}200\ \mu\text{g m}^{-3}$).

[Title Page](#)
[Abstract](#)
[Introduction](#)
[Conclusions](#)
[References](#)
[Tables](#)
[Figures](#)
[⏪](#)
[⏩](#)
[◀](#)
[▶](#)
[Back](#)
[Close](#)
[Full Screen / Esc](#)
[Printer-friendly Version](#)
[Interactive Discussion](#)

Uncertainties in the estimation of organic aerosols volatility

E. Fuentes and
G. McFiggans

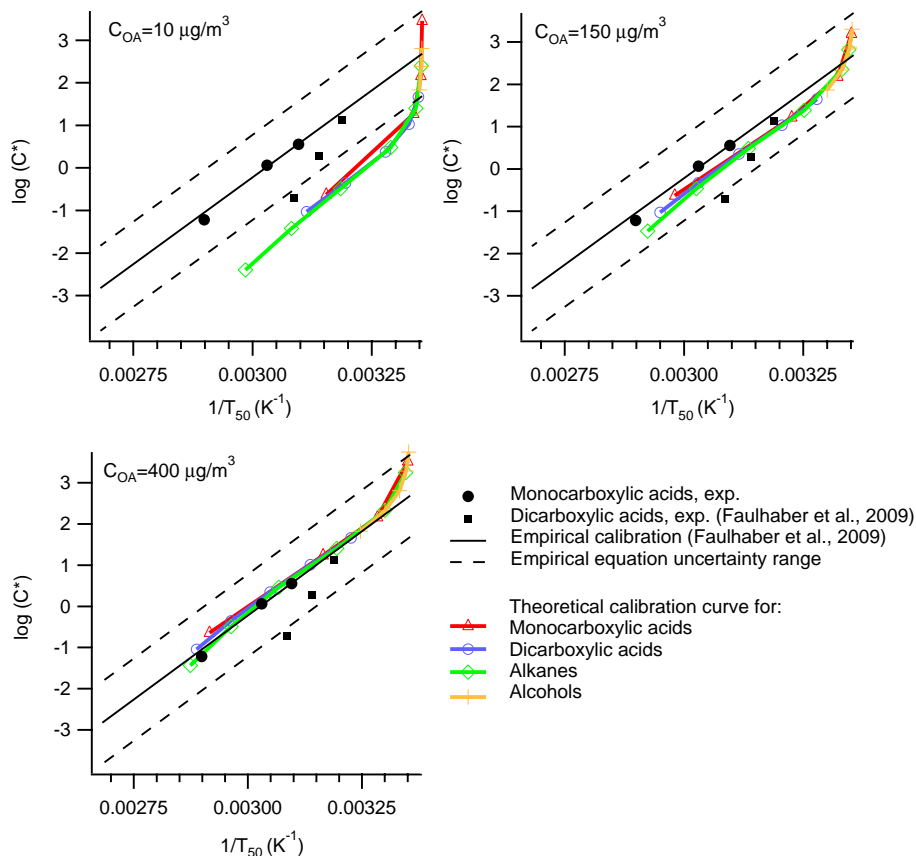


Fig. 11. Theoretical relationship between C_0^* and $1/T_{50}$ for different organic compounds, as derived from Eq. (22) at different aerosol mass loadings. The empirical and theoretical curves overlap for high aerosol loadings, while deviation between the curves is expected for low atmospheric aerosol loadings.

[Title Page](#)
[Abstract](#)
[Introduction](#)
[Conclusions](#)
[References](#)
[Tables](#)
[Figures](#)
[⏪](#)
[⏩](#)
[◀](#)
[▶](#)
[Back](#)
[Close](#)
[Full Screen / Esc](#)
[Printer-friendly Version](#)
[Interactive Discussion](#)

Uncertainties in the estimation of organic aerosols volatility

E. Fuentes and
G. McFiggans

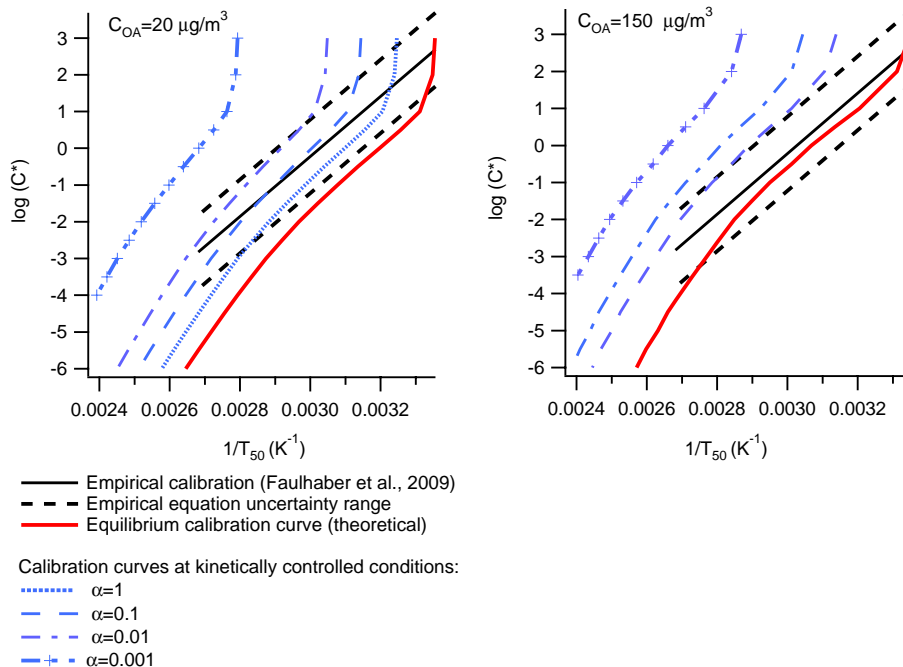


Fig. 12. Deviation of the calibration curve due to equilibrium not being attained in thermodeuder measurements at two different aerosol loadings. T_{50} deviations up to ~ 20 – 30°C , with respect to equilibrium, situate the calibration curve within the uncertainty region of the empirical formulation. Further difference with respect to equilibrium (particularly for $\alpha < 0.01$) leads to significant deviation of the calibration curve with respect to the empirical and theoretical curves.

[Title Page](#)
[Abstract](#)
[Introduction](#)
[Conclusions](#)
[References](#)
[Tables](#)
[Figures](#)
[◀](#)
[▶](#)
[◀](#)
[▶](#)
[Back](#)
[Close](#)
[Full Screen / Esc](#)
[Printer-friendly Version](#)
[Interactive Discussion](#)

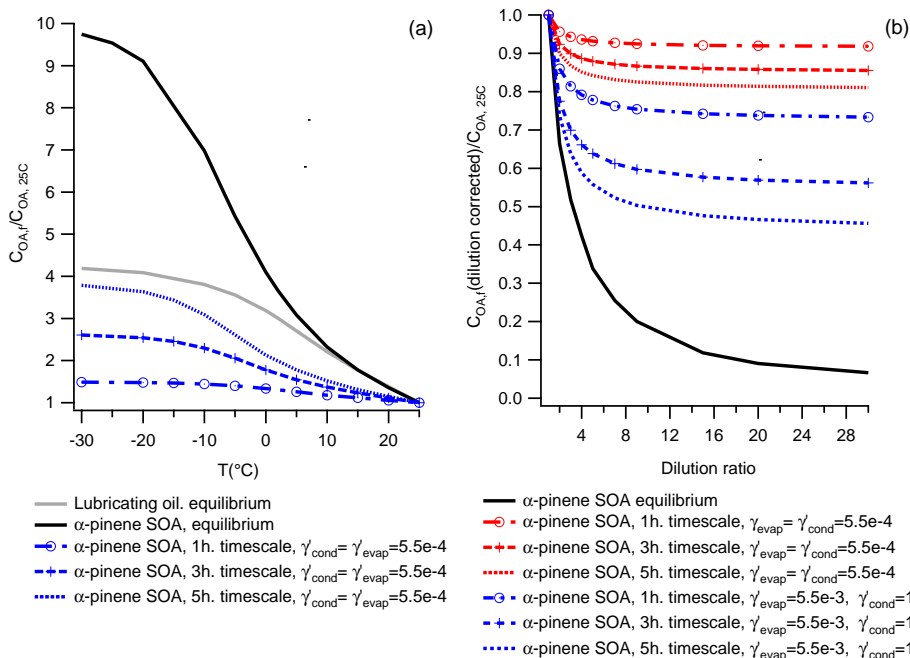


Fig. 13. (a) Condensed mass forming potential of lubricating oil and α -pinene SOA resulting from cooling from initial conditions at $25^{\circ}C$ and $20 \mu g m^{-3}$ aerosol loading. For the α -pinene SOA aerosol, the cases presented are (1) equilibrium, assuming that gas condensation is not affected by the particle phase and (2) non-equilibrium conditions with $\gamma'_{cond} = \gamma'_{evap}$. A strong difference is obtained in the particle mass change estimation, depending on the assumption of condensation being or not affected by the particle glassy state. **(b)** Change in α -pinene SOA aerosol mass resulting from dilution-induced evaporation for the cases of (1) equilibrium (2) non-equilibrium with $\gamma'_{evap} = \gamma'_{cond}$ and (3) non-equilibrium with $\gamma'_{evap} = 5 \times 10^{-3}$ and $\gamma'_{cond} = 1$. While the equilibrium partitioning calculations significantly overestimate the amount of glassy aerosol mass evaporated due to dilution, a large difference in the estimation of aerosol mass is obtained depending on the assumption of effective evaporation coefficient.

Uncertainties in the estimation of organic aerosols volatility

E. Fuentes and
G. McFiggans

Title Page

Abstract

Introduction

Conclusions

References

Tables

Figures

◀

▶

◀

▶

Back

Close

Full Screen / Esc

Printer-friendly Version

Interactive Discussion

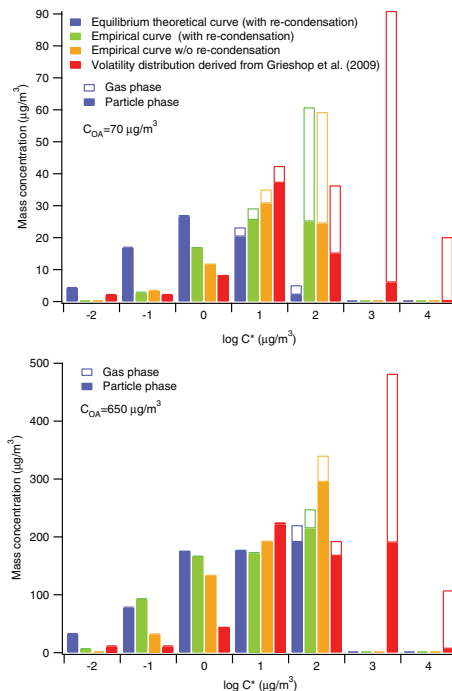


Fig. 14. Volatility distributions derived from lubricating oil thermograms at 70 and 650 $\mu\text{g m}^{-3}$ aerosol loading, using the equilibrium and empirical calibration curve approach. For 70 $\mu\text{g m}^{-3}$ **(a)** the thermogram considerably deviates from equilibrium (Figs. 8 and S5), thus, resulting in the equilibrium calibration approach underestimating the aerosol volatility. The empirical calibration provides a better agreement in this case, due to the calibration curve fortuitously laying on the empirical calibration curve (Fig. S5). For the highest aerosol loading **(b)**, the thermograms are close to equilibrium (Figs. 8 and S5) and the predictions approach the distribution derived using the volatility basic-set distribution by Grieshop et al. (2009).

Uncertainties in the estimation of organic aerosols volatility

E. Fuentes and
G. McFiggans

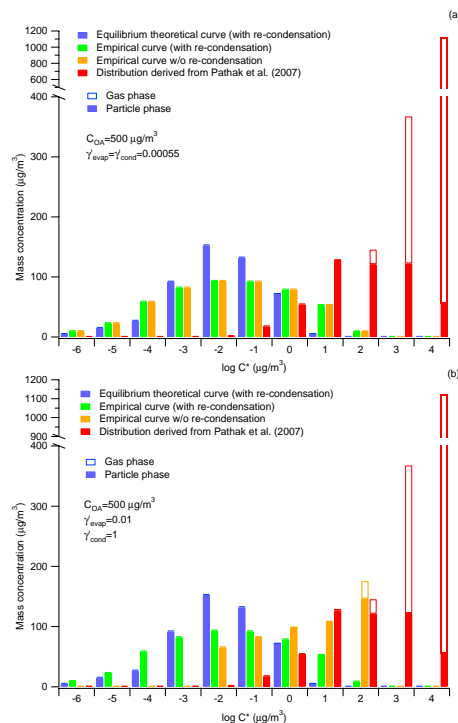


Fig. 15. Volatility distributions derived from α -pinene SOA thermograms at $500 \mu\text{g m}^{-3}$ aerosol loading in comparison with the distribution derived using the parameterisation by Pathak et al. (2007). For case **(a)** the volatility is substantially underestimated due to the thermogram being significantly far from both the equilibrium and the empirical calibration curves region, while in **(b)** the deviation using the calibration curve approach is partly due to significant re-condensation.

[Title Page](#)
[Abstract](#)
[Introduction](#)
[Conclusions](#)
[References](#)
[Tables](#)
[Figures](#)
[◀](#)
[▶](#)
[◀](#)
[▶](#)
[Back](#)
[Close](#)
[Full Screen / Esc](#)
[Printer-friendly Version](#)
[Interactive Discussion](#)

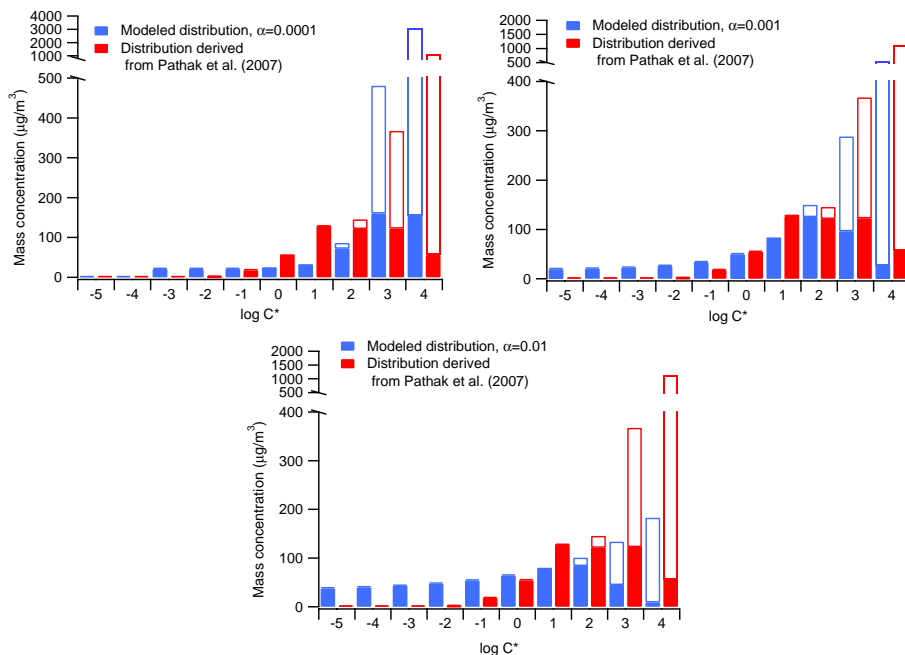
Uncertainties in the estimation of organic aerosols volatilityE. Fuentes and
G. McFiggans

Fig. 16. Volatility distributions derived from α -pinene SOA thermograms at $500 \mu\text{g m}^{-3}$ aerosol loading using the kinetic model approach with different accommodation coefficient values, in comparison with the distribution derived from data by Pathak et al. (2007). The derived distribution is sensitive to the assumption of effective accommodation coefficient, with a shift towards lower volatility for increasing kinetic coefficient.

Title Page

Abstract

Introduction

Conclusions

References

Tables

Figures

◀

▶

◀

▶

Back

Close

Full Screen / Esc

Printer-friendly Version

Interactive Discussion